

Ingvill Reistad

A Review of Fennoscandian Stictochironomus (Diptera: Chironomidae), with the description of a species new to science

Master's thesis in Systematics and Biodiversity (NABIS)

Supervisor: Torbjørn Ekrem

Co-supervisor: Elisabeth Stur

May 2023

Ingvill Reistad

**A Review of Fennoscandian
Stictochironomus (Diptera:
Chironomidae), with the description of
a species new to science**

Master's thesis in Systematics and Biodiversity (NABIS)
Supervisor: Torbjørn Ekrem
Co-supervisor: Elisabeth Stur
May 2023

Norwegian University of Science and Technology
NTNU University Museum
Department of Natural History



Abstract

Chironomidae is one of the most abundant and species rich families of freshwater insects. The genus *Stictochironomus* Kieffer, 1919, belongs to the widely distributed subfamily Chironominae and currently has six named species recorded from Fennoscandia. However, the DNA barcode data of *Stictochironomus* specimens collected in Norway and Finland indicate eight different genetic lineages, excluding *Stictochironomus crassiforceps*. In this study, the Fennoscandian species of the genus *Stictochironomus* are reviewed in an integrative framework, where species boundaries were examined using molecular and morphological data. Phylogenies derived from sequences of the mitochondrial COI, nuclear protein coding AATSI, and PGD DNA markers, as well as the Generalized Mixed Yule Coalescent (GMYC) method, and morphological characters were used to support the delimitation of eight Fennoscandian species. One of these species is new to science and an additional two probably new to science. In this thesis, I describe the species known from Fennoscandia and provide an illustrated identification key to Fennoscandian *Stictochironomus*. To avoid creating a nomen nudum, the new species is not formally named. A lectotype for *Stictochironomus rosenschoeldi* is selected to stabilize future nomenclature of this species.

Sammendrag

Chironomidae, eller fjærmygg på norsk, er en av de mest artsrike og utbredte familiene av ferskvannsinsekter i verden. Under slekten *Stictochironomus* Kieffer, 1919 finnes det seks beskrevne arter i Fennoskandia, men DNA barcode data tyder på at det finnes åtte forskjellige arter her, utenom arten *Stictochironomus crassiforceps*. I dette studiet har slekten *Stictochironomus* blitt revaluert i et integrativt rammeverk, og artsgrenser har blitt testet med molekylære og morfologiske analyser. Fylogener basert på den mitokondrielle markøren COI, de to nukleære proteinkodende markørene PGD og AATSI, 'Generalized Mixed Yule Coalescent' (GMYC) metoden og morfologiske karakterer ble brukt til å støtte opp avgrensningen av åtte arter av *Stictochironomus* i Fennoskandia. I denne avhandlingen breskrives alle artene som er kjent fra Fennoskandia, inkludert minst en ny art og to mulige nye arter for vitenskapen. En illustrert artsnøkkel ble laget. For å unngå opprettelsen av et nomen nudum har ikke den nye arten fått et offisielt navn enda. En lectotype for *Stictochironomus rosenschoeldi* har blitt valgt ut for å stabilisere framtidig nomenklatur for denne arten.

Acknowledgements

This master's thesis was written at the Norwegian University of Science and Technology (NTNU) University Museum, department of Natural History. I want to thank my supervisors, Torbjørn Ekrem and Elisabeth Stur for guiding me through this project with their vast practical and theoretical knowledge of chironomids and taxonomy. I also want to give a special thanks Marko Mutanen, senior curator at the University of Oulu for loaning me twelve specimens of *Stictochironomus* from Finland, and Mohsen Falahati and Aina Mærk Aspaas for giving and advice in the molecular and microscope labs. Finally, I want to thank my fellow students and friends who have provided both emotional support, amazing problem solving skills and theoretical insight during this year.

Table of contents

Introduction	1
Chironomidae	1
<i>Stictochironomus</i> Kieffer, 1919	2
Species concepts and species delimitation	4
Aims and hypothesis.....	5
Material and methods	6
Fieldwork	6
Measurements of morphological characters	7
Illustrations.....	8
DNA extraction and PCR.....	9
Sequence editing and alignment.....	10
Species delimitation.....	11
Results	12
Phylogenetic trees.....	12
Delimitation	16
Morphology.....	16
<i>Stictochironomus maculipennis</i> (Meigen, 1818).....	17
<i>Stictochironomus</i> sp. <i>pictulus</i> I	19
<i>Stictochironomus</i> sp. <i>pictulus</i> II	21
<i>Stictochironomus psilopterus</i> (Edwards, 1935)	23
<i>Stictochironomus rosenschoeldi</i> (Zetterstedt, 1838).....	25
<i>Stictochironomus</i> sp. 2TE	27
<i>Stictochironomus</i> sp. <i>sticticus</i> Norway	29
<i>Stictochironomus</i> sp. 3TE	30
Other species.....	32
Key to male adults of the Fennoscandian <i>Stictochironomus</i> species	34
Discussion	35
Phylogenetic trees.....	35
Delimitation - GMYC.....	36
Morphology.....	37
Future priorities	39
Conclusion	39
References	40
Appendices	44

List of figures

Figure 1 – A photography of a specimen of the species <i>Stictochironomus rosenschoeldi</i> (Zetterstedt, 1838) collected in Finnmark, Norway. Scalebar 2 mm.	2
Figure 2 – Fieldwork in Finnmark: catching <i>Stictochironomus</i> adults with an insect net by Nordvivatnet.	6
Figure 3 – Measurements of length of wing veins Cu, M, R ₁ , R ₂₊₃ and R ₄₊₅ . The specimen depicted has the BOLD specimen ID: Finnmark108 and has been identified as <i>Stictochironomus</i> sp. 2TE. Scalebar 2 mm.	7
Figure 4 – Measurements of the hypopygium. Length of A) tergite IX, B) gonostylus, C) gonocoxite, D) anal point, E) phallapodeme F) transverse sternapodeme and G) inferior volsella. The specimen depicted has the BOLD specimen ID: Finnmark108 and has been identified as <i>Stictochironomus</i> sp. 2TE. Scalebar 300 µm.	8
Figure 5 – Consensus tree from Maximum Likelihood analysis (RAxML) of the concatenated dataset created in CRIPES with default settings, including the DNA markers COI, PGD and AATSI. Branch labels are showing bootstrap values. Tip are labelled with the morphological species identification, and specimen ID as labelled on microscope slides, or as retrieved from BOLD. Scalebar represents genetic distance. All genetic clusters are indicated in the sidebar.	14
Figure 6 – Majority rule consensus tree from MrBayes analysis of the concatenated dataset created in CIPRES with default settings, including the DNA markers COI, PGD and AATSI. Branch labels are showing branch lengths (the mean of the posterior probability density) higher or equal to 70. Tip are labelled with the morphological species identification, and specimen ID as labelled on microscope slides, or as retrieved from BOLD. Scalebar represents genetic distance. All genetic clusters are indicated in the sidebar.	15
Figure 7 – Hypopygium of <i>Stictochironomus maculipennis</i> , the specimen depicted is BOLD specimen ID: TDR-CH95. Scalebar 200 µm.	18
Figure 8 – Hypopygium of <i>Stictochironomus pictulus</i> , the specimen depicted is BOLD specimen ID: ZMUO.024720. Cluster <i>Stictochironomus</i> sp. <i>pictulus</i> I. Scalebar 200 µm.	20
Figure 9 – Hypopygium of <i>Stictochironomus pictulus</i> , the specimen depicted is BOLD specimen ID: ZMUO.025173. Cluster <i>Stictochironomus</i> sp. <i>pictulus</i> II. Scalebar 200 µm.	22
Figure 10 – Hypopygium of <i>Stictochironomus psilopterus</i> , the specimen depicted is BOLD specimen ID: BJ196. Scalebar 200 µm.	24
Figure 11 – Hypopygium of <i>Stictochironomus rosenschoeldi</i> , the specimen depicted is BOLD specimen ID: Finnmark527. Scalebar 200 µm.	26
Figure 12 – Hypopygium of <i>Stictochironomus</i> sp. 2TE, the specimen depicted is BOLD specimen ID: Finnmark108. Scalebar 200 µm.	28
Figure 13 – Hypopygium of <i>Stictochironomus</i> sp. 3TE, the specimen depicted is BOLD specimen ID: ZMUO.024598. Scalebar 200 µm.	31
Figure 14 – Illustrations showing variance of superior volsella in <i>S. pictulus</i> . Specimens A) BOLD specimen ID: ZUMO.024720 and B) BOLD specimen ID: ZUMO.024721 fall within the cluster <i>Stictochironomus</i> sp. <i>pictulus</i> I and specimens C) BOLD specimen ID: ZUMO.025172 and D) BOLD specimen ID: ZUMO.025173 fall within the cluster <i>Stictochironomus</i> sp. <i>pictulus</i> II. For size see figure of hypopygium.	33
Figure 15 – Illustrations showing variance of superior volsella in <i>S. maculipennis</i> . Specimens A) BOLD specimen ID: AT568, B) BOLD specimen ID: TRD-CH95, C) BOLD specimen ID: TRD-CH321. For size see figure of hypopygium.	33

List of tables

Table 1 – Primers used for DNA amplification.....	9
--	---

Introduction

Chironomidae

Chironomidae is the most abundant and species rich family of aquatic insects, with more than 6000 species described worldwide (Ashe & O'Connor, 2009, 2012), and over 1200 species described in Europe (Sæther & Spies, 2010). The estimated number of species worldwide is 15000 (Armitage et al., 1995), suggesting that less than half the species diversity in the world has been described. Adaptations to extreme environments of temperature, salinity, depth and pH has allowed them to inhabit every continent of the Earth. This makes chironomids the most widely distributed family of free-living holometabolous insects, ranging all the way from Ellesmere Island in the north to the mainland of Antarctica in the south (Armitage et al., 1995). Nevertheless, most people are unaware that this large family even exists, perhaps with the exception of avid fly fishers that use lures representing chironomid pupa when fishing in freshwater. In English, chironomids are called non-biting midges or lake flies, which are fitting names that describes parts of their ecology and life history.

All holometabolous insects have a complete metamorphosis with four life stages: egg, larva, pupa, and imago. Chironomids spend the majority of their lives as larvae, and this life stage can last from a few weeks up to several years (Butler, 1982; Lindegaard-Petersen, 1971). Most larvae live in aquatic environments of any form, from glacial rivers high up in mountains to the seashores, and some species are even marine. However, some species have a semi aquatic larval stage in moss and other humid substrates, and a few species are even fully terrestrial living in soil, dung and fungi (Armitage et al., 1995; Cranston et al., 1989; Oliver, 1971). The larvae feed on algae, algae-detritus, detritus, and some are even carnivorous. After four larval instars they start forming a pupa. This process can be triggered by daylength, temperature and other external factors. The pupal stage is very brief and only lasts up to a few days before the chironomid emerges as an imago. The adults usually live a few weeks, and their only goal is to reproduce and lay eggs (Oliver, 1971). They often form swarms near the body of water in which they emerged, as a part of their mating behavior.

Sometimes there is an enormous number of chironomids emerging at once, forming such dense swarms that they become a nuisance to humans. Recorded incidents include chironomid swarms so dense they fly into the ears, nose and eyes, making it hard to breathe and really uncomfortable to be outdoors (Grodhaus, 1963). In Japan there has been cases of dead chironomids covering roads in a slimy fishy smelling layer making it dangerous to drive. The abundance and species richness of chironomids is not only a bad thing. They play a crucial role in the ecosystem as consumers of organic matter in aquatic environments, and as a major food source for other consumers in both aquatic and terrestrial food webs (Armitage et al., 1995). Chironomids have been used in

freshwater biomonitoring and as water quality indicators for over a hundred years (Cranston et al., 1989). Being present on every continent, they are useful for tracking biogeographic trends and processes (Porinchu & MacDonald, 2003). In order to protect and manage ecosystems and wildlife it is crucial that as much as possible is known about the species composition of the ecosystem, their abundance and ecology. Mapping species diversity is thus, in some way, beneficial to everyone.

Stictochironomus Kieffer, 1919



Figure 1 – A photograph of a specimen of the species *Stictochironomus rosenschoeldi* (Zetterstedt, 1838) collected in Finnmark, Norway. Scalebar 2 mm.

The genus *Stictochironomus* (Figure 1) belongs to the subfamily Chironominae and shares the typical characteristics of this group. The adults are quite large, with a wing length of 2.5-4.7 mm. The body is light brown to dark brown. There is dark spot on the wing membrane surrounding RM, and some species have a pattern of an additional 4-5 spots on the wing. The legs sometimes have alternating light and dark bands of rings, fore tibia has scale, otherwise fused tibial combs with 1-2 spurs. The thorax has a conical scutal tubercle. *Stictochironomus* is one of few genera within the subfamily Chironominae that has movable gonostyli. Characters on the wing, thorax and male genitalia are useful for species identification of adult specimens (Cranston et al., 1989).

The pupae are quite large, 7-10 mm long. *Stictochironomus* can be identified within the tribus Chironomini by the combination of these characters: they have a plumose thoracic horn together with anterior horn, on tergite II-VI there are transverse bands of shagreen, the anal combs are robust and longitudinal, there is a lack of dorsal setae on the anal lobes, the frontal setae are long and robust, and the cephalic tubercles are well developed. *Stictochironomus* pupae are very similar to those of *Tribelos*, but they differ in that *Tribelos* have 1 very long dorsal seta on each anal lobe, the frontal setae are short and slender, and they have 5 LS setae on segment VIII, not 4 like *Stictochironomus* (Pinder & Reiss, 1986).

The larvae are large, up to 14 mm long. They are red and have 2 pairs of separate eyes. In addition the following combination of characters can be used to identify *Stictochironomus* larvae: antennae are 6-segmented with alternate Lauterborn organs; the dorsal tooth of the mandible and all of the mental teeth are dark; the 4 median teeth of the mentum are much higher than the 6 pairs of lateral teeth; and the central pair is much more slender and lower than the outer pair. Larvae living in sand often have strongly worn mouthparts and it can be difficult to use these characters for identification (Epler et al., 2013).

Stictochironomus species are considered aquatic, as their immature stages (eggs and larvae) can be found in profundal soft sediments and littoral sand of oligotrophic to mesotrophic lakes, and in sandy sediments of streams and slow flowing rivers (Cranston et al., 1989; Epler et al., 2013). Adults do not usually migrate far from the body of water from which they emerged and can often be found in vegetation near the shore (Figure 2) (Armitage et al., 1995; Cranston et al., 1989; de Jong et al., 2014; Stur & Ekrem, 2020). *Stictochironomus* can be found in every geographic region except Antarctica and South America, but the known diversity is highest in North America, Europe South Africa, and Japan. Worldwide there are currently about 50 described species (Thompson et al., 1999), six of which can be found in Fennoscandia (Schnell & Aagaard, 1996; Stur & Ekrem, 2020; Sæther & Spies, 2010): *Stictochironomus crassiforceps* (Kieffer, 1921), *Stictochironomus maculipennis* (Meigen, 1818), *Stictochironomus pictulus* (Meigen, 1830), *Stictochironomus psilopterus* (Edwards, 1935), *Stictochironomus rosenschoeldi* (Zetterstedt, 1838) and *Stictochironomus sticticus* (Fabricius, 1781).

Although Kieffer (1919) described the genus *Stictochironomus* in 1919, several of the species had already been described and were classified first within *Tipula* and later *Chironomus* (Fabricius, 1781; Meigen, 1818; Meigen, 1830). The identity of within *Stictochironomus* has not always been unambiguous. There has especially been some confusion regarding *S. sticticus* and *S. pictulus*. Fabricius (1781:407) described *Tipula stictica* (*S. sticticus*) as a species with dark thorax, light bands on the abdomen and a single dark spot in the middle of the wing. In 1818, Meigen (1818:37) published a description of a specimen he had received from Hoffmann and identified it as *Chironomus sticticus* (Fabricius, 1781). Hoffmann had labelled the specimen as *ch. pictulus* but had never published a description nor the name. Meigen described the wing pattern of the specimen as having three gray spots in addition to the central black spot. He noticed that the wing pattern was different from Fabricius' description of *Tipula stictica* sensu Fabricius (1781:407) and assumed that Fabricius might have overlooked this detail. Some years later, Meigen (1830:244) realized that he had misidentified Hoffmann's specimen as *Chironomus sticticus* (Fabricius, 1781), and that it was a separate species. Meigen named Hoffmann's specimen *pictulus*. In the same publication Meigen corrected a spelling mistake (*Chir. strictus*) and synonymized *Chironomus histrio* with *Chironomus sticticus* (Fabricius, 1781).

Species concepts and species delimitation

Species are one of the fundamental units in biology (Dobzhansky, 1982; Mayr, 1999), but the question of what ultimately defines a species has long been one of the most controversial topics in biology. The issue of species delimitation has been confused with the definition of species as a concept (De Queiroz, 2007). There are at least 26 recognized species concepts (Wilkins, 2006), however none of these singlehandedly work as a universal definition across all phyla. Together, all of the definitions conform to a primary concept that is now universally accepted: species is a metapopulation evolving along a single lineage. In order to delimit species using the primary concept there is a need for operational or secondary species criteria (De Queiroz, 2007). These secondary species concepts rely on different criteria depending on the different concepts, each having advantages and disadvantages that should be considered in the light of the taxonomic group in question. Keeping this in mind, an integrative approach to species delimitation will arguably take advantages of different criteria and possibly reduce the disadvantages of single species concepts. Integrative taxonomy aims to integrate data from multiple perspectives in order to delimit the units of life's diversity (Dayrat, 2005; Garraffoni et al., 2019). In this study, the morphological and phylogenetic species concepts are used.

The morphological species concept as adapted by Cronquist (1978) is defined as "the smallest groups that are constantly and determinedly distinctive and distinguishable by average means." Morphological characters have been used to delimit species ever since Linnaeus first started describing and naming species. Delimiting species by this definition includes qualitative

comparisons and quantitative measurements of diagnostic features. In the case of Chironomidae, all you need to study and describe species is experience, literature, and a microscope. Sometimes, however, the level of expertise needed to distinguish species morphologically is not possible to reach without years of practice, which can be problematic (Aldhebiani, 2018). Other problems is that the morphological species concept is not able to distinguish cryptic species, geographic variation among populations or polymorphism within populations.

With the access to better and cheaper technology for DNA extraction and sequencing, delimiting species with genetic characters is quickly becoming a common method. With a morphologically difficult taxon like Chironomids, studying the molecular data is an effective way to reveal species diversity that is hidden morphologically. The phylogenetic species concept is defined by Cracraft (1989) as “an irreducible cluster of organisms diagnosably distinct from other such clusters, and within which there is a parental pattern of ancestry and descent”. Numerous statistical methods have been developed to analyze molecular data and delimit species with different assumptions and parameters. A problem though, is how to choose which genetic character to use as different markers have different qualities and substitution rates. This problem can be avoided by using several different markers and multiple delimitation methods to verify the results. One method commonly used is the Generalized Mixed Yule-Coalescent (GMYC) (Pons et al., 2006), which delimits species with a maximum likelihood approach by fitting within- and between-species branching models to reconstructed gene trees. This method, however, tends to overestimate the number of operational taxonomic units (OUTs). Another approach, used in the Barcode of Life Data Systems (BOLD), involves the delimiting of barcode clusters through comparing genetic similarity between sequences followed by analyses of genetic distances to neighboring clusters in an iterative manner. The clusters are given unique names (Barcode Identification Numbers, BINs) and are regarded as proxies for species (Ratnasingham & Herbert, 2007). For chironomids BINs are found to overestimate divergence at the species-level (Ekrem et al., 2018).

The DNA barcoded Norwegian, Swedish and Finnish specimens of *Stictochironomus* have been assigned nine Barcode Index Numbers (BINs) in BOLD. These BINS form eight well separate clades, and three of these clades could potentially represent new species to science as they so far could not be associated with described taxa. To clarify the status of these lineages, original descriptions and type specimens of known species must be consulted, and the morphological and molecular characteristics described and analyzed.

Aims and hypothesis

The aim of this study is to review the species of the genus *Stictochironomus* found in Norway and make a cohesive conclusion as to which species exist here now. The main hypothesis is that the genetic clusters observed in the COI DNA barcode data of the interim name *Stictochironomus* sp. 2TE, as well as one of the two clusters identified and

S. sticticus / *Stictochironomus* sp. 3TE, and one of the two clusters identified as *S. pictulus* represent distinct species that are new to science.

Through analyses of morphological and molecular characters, diversity at the species level was assessed in an integrative approach. The delimitation method applied to the genetic markers was GMYC. Literature and selected types were reviewed to determine whether these species are to be described as their own species or fit into one of the preexisting species. In addition, I have made an illustrated identification key to the Fennoscandian species of *Stictochironomus*.

Material and methods

Fieldwork

Chironomids were collected from and by lakes in Trøndelag during May 2022 and in Vestre Jakobselv and Vadsø in Finnmark during early June 2022. The adult specimens were collected using sweep-nets in vegetation near lakes or ponds and stored in 85% ethanol as shown in Figure 2. Larvae were collected from soft, profundal sediments with nets by kick sampling, and sieved through different sized meshes (first 5 mm and last 250 µm) to separate larvae and pupae from the sediment. Some of the larvae and pupa were kept in small containers and brought to the laboratory for emergence. This method allows for comparing all the different life stages between species and increases the confidence in species identification and species delimitation. The rest of the larvae and pupae were fixed in 96% ethanol. All samples were labelled appropriately and kept cool in a fridge at a constant temperature until further studied. Borrowed fresh material was collected in various localities in Finland during May-July 2015 with Malaise traps.



Figure 2 – Fieldwork in Finnmark: catching *Stictochironomus* adults with an insect net by Nordvivatnet.

Measurements of morphological characters

The descriptions of each species' morphology is adapted from the Holarctic keys of Wiederholm (Cranston et al., 1989; Epler et al., 2013; Pinder & Reiss, 1986).

The specimens from Finland, specimens stored in alcohol at NTNU University Museum and a selection of collected specimens from Finnmark were mounted on microscopy slides following standard procedures as described in Cranston et al. (1989). See (Supplementary table B1) to view specimens included in the study. The specimens were dissected by separating the antennae, head, wings, legs, abdomen and thorax from each other. Potassium hydroxide (5-10% solution) was used to remove soft insides of the head and abdomen, leaving only the exoskeleton. The antennae and wings, legs, head, and abdomen were embedded in drops of Euparal and carefully arranged before applying the cover slips. The thorax was stored in 96% alcohol until DNA was extracted, and then mounted together with the rest of the specimen.

The slide mounted specimens were examined and identified using a Leica compound microscope (LEICA DM6000B) and measured using the Leica Application Suite X (LAS X). The morphological analysis included quantitative measurements and qualitative comparisons of diagnostic characters. An overview of the result can be viewed in Table 1. The terminology of morphology used in this study follow Sæther (1980). Characters on the wing and hypopygium were measured respectively according to Figure 3 and Figure 4. The rest of the characters were measured according to Soponis (1977).

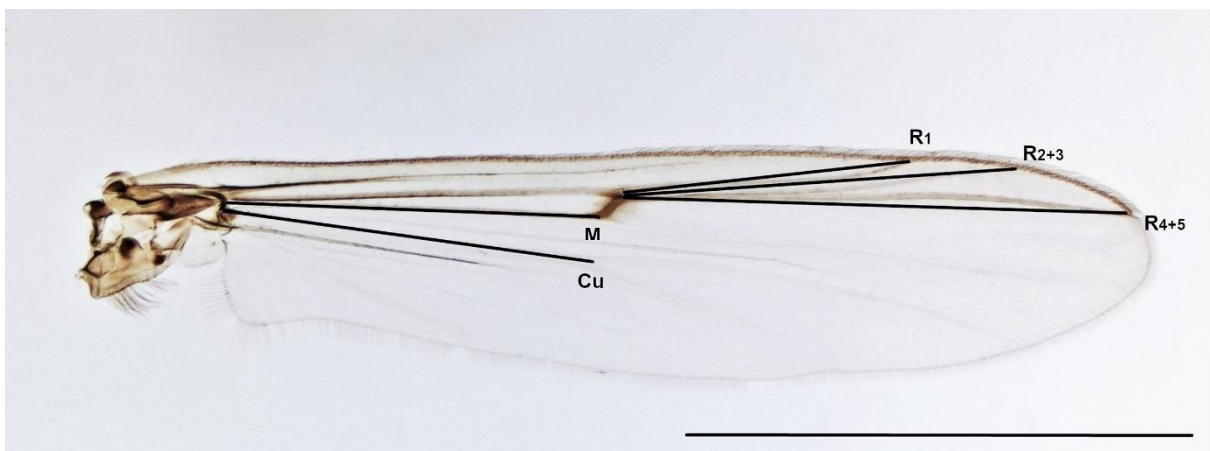


Figure 3 – Measurements of length of wing veins Cu, M, R₁, R₂₊₃ and R₄₊₅. The specimen depicted has the BOLD specimen ID: Finnmark108 and has been identified as *Stictochironomus* sp. 2TE Scalebar 2 mm.

Characters measured and counted on the wings were the length of wing vein R, R₁, R₂₊₃, R₄₊₅, M, Cu (Figure 3), total length of the wing from arculus to tip, the width of the wing, number of setae on wing vein R, R₁, R₂₊₃, R₄₊₅, M, Cu, Cu₁, Cu₂, An and false vein, squama and brachiolum.

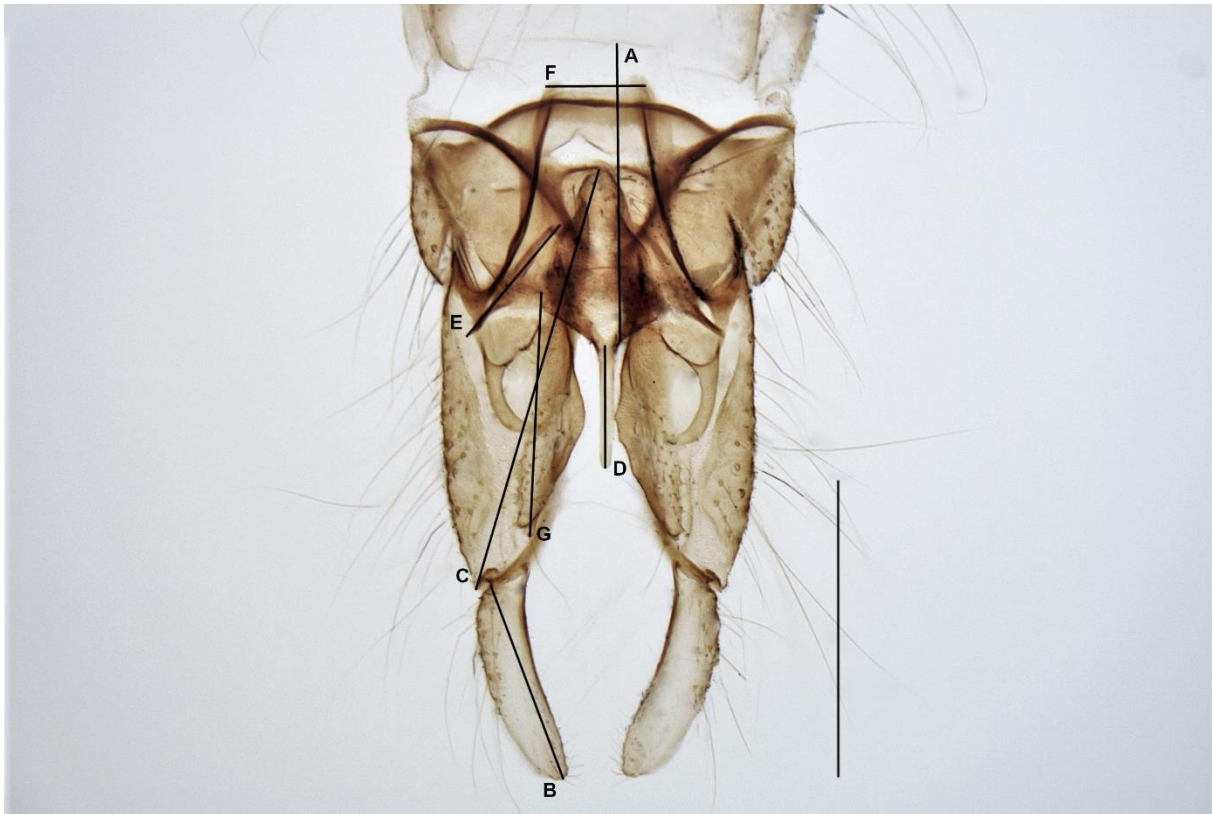


Figure 4 – Measurements of the hypopygium. Length of A) tergite IX, B) gonostylus, C) gonocoxite, D) anal point, E) phallapodeme F) transverse sternapodeme and G) inferior volsella. The specimen depicted has the BOLD specimen ID: Finnmark108 and has been identified as *Stictochironomus* sp. 2TE. Scalebar 300 μ m.

On the hypopygium, the lengths of tergite IX, gonostylus, gonocoxite, anal point, phallapodeme, transverse sternapodeme and inferior volsella were measured (Figure 4). The number of setae on superior volsella and median volsella was counted, and the shape of superior volsella was recorded. On the head, the length of flagellomeres and the longest antennal setae, width of head, pedicel, distance between the eyes, and length of the palpomeres was measured (Soponis, 1977).

Characters measured on the legs were length of femur, tibia, tarsus 1-5 on the foreleg, midleg and hindleg. On the foreleg, the tibial spur was measured (Soponis, 1977). On all three legs, bristle ratio, LR (tarsus1/tibia), BV (femur + tibia + tarsus 1 / sum tarsus 2-5) and SV (femur + tibia / tarsus 1) was calculated. On the thorax, the number of dorsocentrals, scutellars and prealars were counted.

Illustrations

Illustrations of the hypopygium of a specimen from each genetic cluster was made by studying the microscope slides through a microscope with a camera lucid. In addition, detail drawing were made of the superior volsella of all the *S. pictulus* specimens. First a sketch was made with a graphite pencil on a piece of A3 sized paper, then a detailed

illustration was made with a felt tip pen on tracing paper. The illustration was scanned and retouched in GNU Image Manipulation Program (GIMP) v2.10.32.

DNA extraction and PCR

The COI DNA barcode sequences from some of the borrowed mounted specimens were previously barcoded and obtained through BOLD (Ratnasingham & Herbert, 2007), see Supplementary Table B1. The DNA was extracted from the specimens non-destructively using the Qiagen DNeasy Blood and Tissue Kit, following the recommended protocol for animal tissue samples. Thorax and sometimes abdomen were air-dried on a piece of paper before being placed in a 1.5 mL centrifuge tube with 180 μ L buffer ATL and 20 μ L proteinase K. The tubes were vortexed thoroughly before being placed in a rotating incubator at 56°C for lysis overnight for approximately 15 hours. When the lysis was complete, 200 μ L Buffer AL and 200 μ L molecular grade ethanol (100%) was added. The tubes were vortexed in between each step. The buffer mixture was pipetted into a DNeasy Mini spin column with a 2 mL collection tube. The thorax was washed two times with water and then stored in a tube with 96% alcohol until mounted with the rest of the specimen. The spin column was washed first with 500 μ L buffer AW1 then with 500 μ L buffer AW2. Centrifuged at 6000 x g (8000 rpm) for 1 minute between each step, and 20,000 x g (14,000 rpm) for 3 minutes at the last step to dry the membrane. The spin column was placed in a new 1,5 mL lo-bind Eppendorf tube, 100 μ L Buffer AE was added onto the membrane, incubated for 1 minute then centrifuged at 6000 x g (8000 rpm) for 1 minute to elute. The final flow through containing DNA was stored in a refrigerator.

The genetic markers targeted for DNA amplification was the mitochondrial COI, and the three nuclear markers CAD1, AATSI and PGD using mostly previously published primers (Table 1). These markers have been used successfully on chironomids in the past (Cranston et al., 2012; Lin et al., 2018).

Table 1 – Primers used for DNA amplification.

Gene segment	Oligo name	Oligo sequence (5'-3')	Reference
Cytochrome <i>c</i> oxidase subunit I (COI)	LCO1490	GGTCAACAAATCATAAAGATATTGG	Folmer et al. (1994)
	HCO2198	TAAACTTCAGGGTGACCAAAAAATCA	Folmer et al. (1994)
Carbamoyl phosphate synthetase 1 (CAD1)	54F	GTNGTNTTYCARACNGGNATGGT	Moulton and Wiegmann (2004)
	405R	GCNGTRTGYTCNGGRTGRAAYTG	Moulton and Wiegmann (2004)
Alanyl- tRNA synthetase 1 (AATS1)	A1-92F	TAYCAYCAYACNTTYTYGARATG	Regier et al. (2008)
	A1-244R	ATNCCRCARTCNATRTGYTT	Su et al. (2008)
6- phosphogluconate dehydrogenase (PGD)	PGD-2F	GATATHGARTAYGGNGAYATGCA	Regier et al. (2008)
	PGD-3R	TRTGIGCNCCRAARTARTC	B. Cassel unpublished

For COI, AATSI and only a few of the PGD and CAD1, using the Qiagen Multiplex PCR master mix yielded good results. The PCR reactions were prepared in volume of 25 μ L, containing 12,5 μ L Qiagen Multiplex PCR Master Mix (2x), 2,5 μ L 2 μ M primer mix, 8 μ L water (ddH₂O) and 2 μ L DNA. Fragments of COI were amplified with an initial

denaturation step of 95°C for 3 min, followed by 35 cycles of 94°C for 30 s, 48°C for 30 s, 72°C for 1 min, and extension at 72°C for 7 min. Fragments of AATSI, CAD1 and PGD were amplified with a three-step touchdown program with an initial denaturation step of 98°C for 10 s, then 94°C for 1 min followed by 5 cycles of 94°C for 30 s, 52°C for 30 s, 72°C for 2 min, then 7 cycles of 94°C for 30 s, 51°C for 1 min, 72°C for 2 min and 37 cycles (sometimes lowered to 30 cycles) of 94°C for 30 s, 45°C for 20 s, 72°C for 2 min 30 s and one final extension at 72°C for 3 min.

It was challenging to get good results from all the specimens of the segments CAD1 and PGD using the Multiplex PCR master mix. Therefore, a number of DNA concentrations and thermocycling programs were tested on these specimens using Takara ExTaq hot start version.

The PCR reactions that yielded the best results for CAD1 were prepared in volume of 25 μ L, containing 2,5 μ L buffer, 2,0 μ L dNTPs, 1,0 μ L 10 μ M primer1, 1,0 μ L 10 μ M primer2, 14,3 μ L water (ddH₂O), 0,2 μ L Takara ExTaq hot start version and 4,0 μ L DNA. CAD1 was amplified with a three-step touchdown program with an initial denaturation step of 98°C for 10 s, followed by 5 cycles of 94°C for 30 s, 57°C for 30 s, 72°C for 1 min 30 s, then 5 cycles of 94°C for 30 s, 53°C for 30 s, 72°C for 1 min 30 s and 35 cycles of 94°C for 30 s, 45°C for 30 s, 72°C for 1 min 30 s and one final extension at 72°C for 10 min.

For PGD, the PCR reactions that yielded the best results were prepared in volume of 25 μ L, containing 2,5 μ L buffer, 2,0 μ L dNTPs, 1,0 μ L 10 μ M primer1, 1,0 μ L 10 μ M primer2, 16,3 μ L water (ddH₂O), 0,2 μ L Takara and 2,0 μ L DNA. PGD was amplified with a three-step touchdown program with an initial denaturation step of 98°C for 10 s, then 94°C for 1 min, followed by 5 cycles of 94°C for 30 s, 52°C for 30 s, 72°C for 2 min, then 7 cycles of 94°C for 30 s, 51°C for 1 min s, 72°C for 2 min and 30 cycles of 94°C for 30 s, 45°C for 20 s, 72°C for 2 min 30 s and one final extension at 72°C for 3 min.

The amplified DNA was visualized by electrophoresis on a 2% agarose gel using SYBR Safe DNA Gel Stain for fluorescence under blue light, and 6x tri track loading buffer with the amplified DNA in the wells. Amplified DNA was stored in a freezer.

Before sequencing, the amplified DNA were purified using 1 μ L ExoSAP-IT (Applied Biosystems) and incubated in a PCR machine at 37°C for 15 min and 80°C for 15 min, removing excess primers and unincorporated nucleotides enzymatically. The Amplified DNA were sent to Eurofins Genomics using the PlateSeq Kit DNA together with the recommended volume of prepared primers for bi-directional Sanger sequencing. The sequences were added to the BOLD database.

Sequence editing and alignment

Sequences were first edited and assembled using the Staden package (Bonfield et al. 1995). However, not all sequences were successfully aligned to create a consensus for the forward and reverse read, especially for the markers CAD1 and PGD. Many of these

sequences were of good enough quality to be edited and assembled using Geneious software v.8.1.9, but some sequences had too poor quality and were discarded. All the successfully assembled consensus sequences were examined, aligned and further corrected using MEGA II (Kumar et al., 2018) while viewing chromatograms in Geneious. The identity of the specimens collected in Finnmark were verified by blasting the NCBI GenBank through MEGA II. The outgroup was selected to be two specimens of the chironomid genus *Sergentia* and one specimen of the genus *Microtendipes* (Supplementary Table B1). *Sergentia* is closely related to *Stictochironomus*, and *Microtendipes* is not as closely related but like the other two genera it is also within the tribe Chironomini (Cranston et al., 2012). A specimen of the genus *Protanypus* was also sequenced. However, *Protanypus* is of a different subfamily: Diamesinae, and the branches leading from *Protanypus* were so long it made the rest of the tree illegible. The *Protanypus* sequence was discarded. COI sequences of the previously barcoded Fennoscandian species, sequences from the species *S. unguiculatus* from Canada and *S. sticticus* and *S. akizukii* from Japan were retrieved from BOLD and integrated with the COI sequences that were amplified for this study (Supplementary Table B1).

The sequences were aligned using ClustalW with a gap opening penalty of 15 and gap extension penalty of 6.66. The reliability of alignments were tested by translating to amino acid level and checking for stop codons. The alignment was trimmed at the ends by removing primers and superfluous bases.

Species delimitation

Phylogenetic analysis were conducted using Maximum Likelihood in the software Randomized Axelerated Maximum Likelihood (RAxML) (Stamatakis, 2014) with default settings, and Bayesian approaches in the software MrBayes (Ronquist et al., 2012) though CIPRES (Miller et al., 2010). A concatenated dataset of all successful sequences was generated in MEGA II. One phylogenetic tree of the concatenated dataset was created with RAxML, and one with MrBayes and edited in FigTree v.1.4.4. All bootstrap values less than 85 and values within highly supported branches within clades were removed in the concatenated RAxML tree. Probability values lower than 70 were removed from branches of the MrBayes tree.

The Generalized Mixed Yule-Coalescent (GMYC) was used for species delimitation analyses. An ultrametric tree was created using the software BEAST v.2.4.7 (Bouckaert et al., 2014). The high-performance library BEAGLE v.4.0.0 (Ayres et al., 2012; Suchard & Rambaut, 2009) was installed to perform the core calculations. The sequence file (NEXUS format) was imported into BEAUTi. Substitution model was decided by running the sequence file in the software jModels2 v.2.1.8 (Darriba et al., 2012; Guindon & Gascuel, 2003). The additional package standard substitution models v.1.0.1 (SSM) package (Bouckaert & Xie, 2017) was downloaded. The best substitution models were TMP2uF+G for COI; TIM2+G for PGD; and TIM3+G for AATSI. The settings for

generating XML files in BEAUTi were the best substitution model for each marker, gamma category count 4 and shape 1.0, strict clock model, coalescent constant population (Kingman, 1982) and 10000000 chain lengths for Markov chain Monte Carlo (MCMC). The XML files were imported to beast and run three separate times for each marker with a random seed and permission to overwrite files. The Effective Sample Size (ESS) values were checked with the program TRACER (Rambaut et al., 2018). The three .log and .trees files for each marker were combined using the program LogCombiner by resampling states at the lower frequency of 3000 and converting numbers from scientific to decimal notation. A consensus tree was created by constructing a maximum clade credibility (MCC) tree using the program TreeAnnotator. The consensus trees were inspected in FigTree v.1.4.4. GMYC was run in R studio (R Core Team, 2019) with the packages splits (Ezard et al., 2021) and ape (Paradis, 2019).

Results

DNA was extracted and sequenced from a total of 35 specimens: 31 specimens of *Stictochironomus*, one *Microtendipes* and two *Sergentia* specimens as outgroup. The last specimen proved to be of the genus *Protanypus*, and since this genus is not closely related to *Stictochironomus* it was removed from the outgroup and alignments. The markers COI and AATSI amplified successfully for all specimens, and PGD amplified successfully for 23 specimens. The specimens removed from the PGD alignment because of bad signals were *S. maculipennis* TRD-CH95 and Finnmark202, *Stictochironomus* sp. 2TE Finnmark385, and *S. rosenschoeldi* Finnmark527, ZUMO.024303, NORIR02, NORIR06 and NORIR11. The sequences of the marker CAD1 were of such low and variable quality that it was not possible to extract long enough segments that were useful for species delimitation analysis nor phylogenetic analyses. In the final alignment of COI there were 70 sequences with a total length of 654 base pairs (bp), 230 variable sites and 203 parsimony informative sites. The PGD alignment included 23 sequences with a maximum length of 757 bp, as many of the sequences had to be trimmed down to ensure high quality. There were 292 variable sites, and 162 parsimony informative sites. The AATSI alignment included 31 sequences with a length of 259 to 403 bp, 145 variable sites and 104 parsimony informative sites.

Phylogenetic trees

The results from all the phylogenetic analyses (both the individual marker RAxML trees of COI (Supplementary Figure A1), PGD (Supplementary Figure A2) and AATSI (Supplementary Figure A3), and the concatenated RAxML (Figure 5) and MrBayes (Figure 6)) show that the specimens are always assigned into the same genetic clades: *maculipennis*, *Stictochironomus* sp. *pictulus* I, *Stictochironomus* sp. *pictulus* II, *S. psilopterus*, *S. rosenschoeldi*, *Stictochironomus* sp. *sticticus* Norway, *Stictochironomus*

sp. 3TE and *Stictochironomus* sp. 2TE. The genetic distance and the relationships between the clusters varies depending on the marker and method used. However, common for all the trees is that *S. rosenschoeldi* is the most genetically divergent from the outgroup.

The RAxML tree constructed from the concatenated dataset (Figure 5) shows that all the clades are very well supported by high bootstrap values, as the majority of the branches leading to the clades have a bootstrap value of 100. The genetic distance between the clades is large. Within the clades, the genetic distance is low, except for within *Stictochironomus* sp. *pictulus* I. The PGD sequences of the two *Stictochironomus* sp. *pictulus* I specimens were not the best quality, which might explain the large intraspecific difference in the tree (Supplementary Figure A2).

The MrBayes tree constructed from the concatenated dataset (Figure 6) assign the specimens to well supported clades. However, there is a unresolved group of *S. maculipennis*, *Stictochironomus* sp. *pictulus* Japan, *Stictochironomus* sp. 3TE and *Stictochironomus* sp. *pictulus* II.

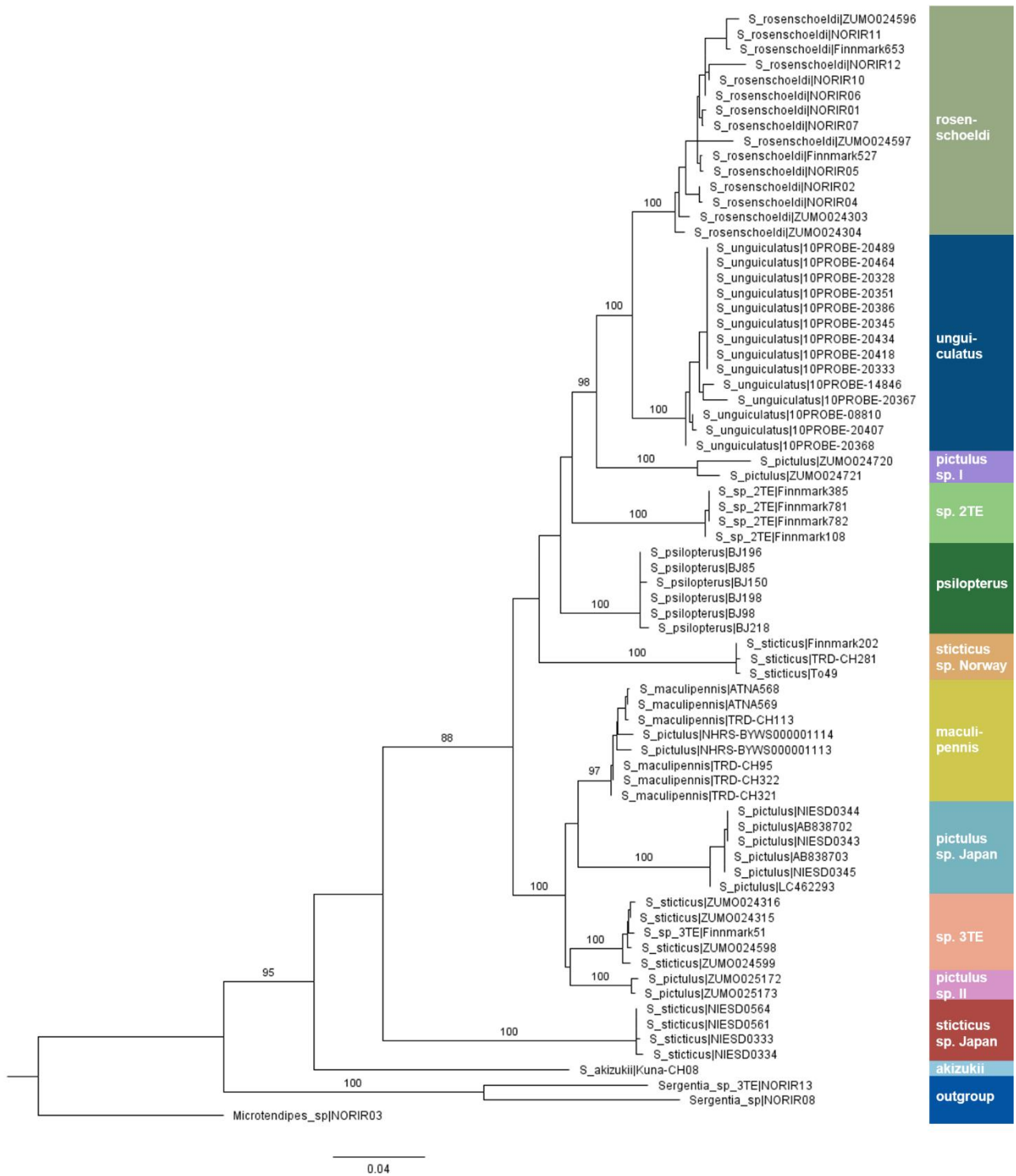


Figure 5 – Consensus tree from Maximum Likelihood analysis (RAxML) of the concatenated dataset created in CRIPES with default settings, including the DNA markers COI, PGD and AATSI. Branch labels are showing bootstrap values. Tip are labelled with the morphological species identification, and specimen ID as labelled on microscope slides, or as retrieved from BOLD. Scalebar represents genetic distance. All genetic clusters are indicated in the sidebar.

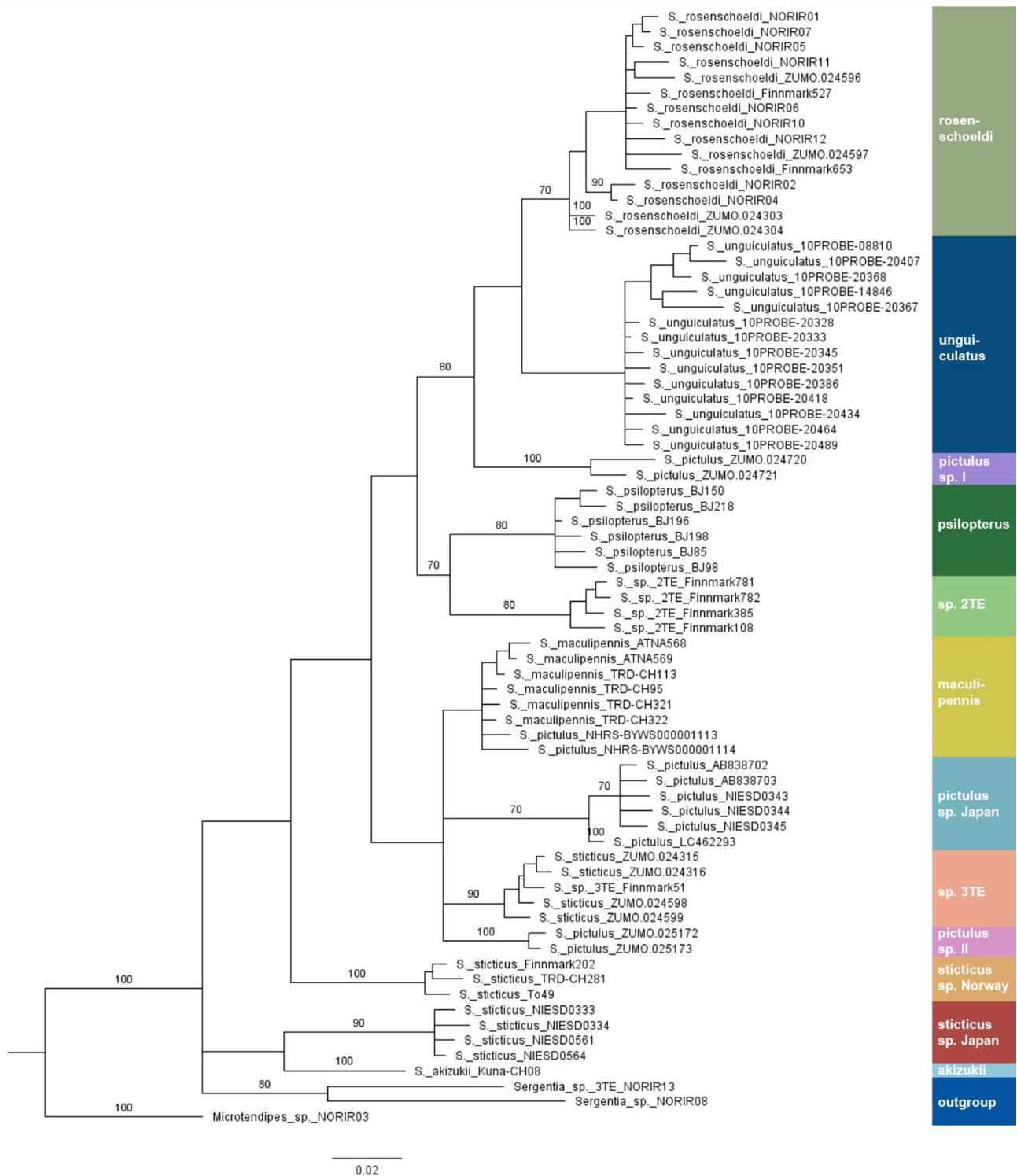


Figure 6 – Majority rule consensus tree from MrBayes analysis of the concatenated dataset created in CIPRES with default settings, including the DNA markers COI, PGD and AATSI. Branch labels are showing branch lengths (the mean of the posterior probability density) higher or equal to 70. Tip are labelled with the morphological species identification, and specimen ID as labelled on microscope slides, or as retrieved from BOLD. Scalebar represents genetic distance. All genetic clusters are indicated in the sidebar.

Delimitation

The complete dataset of all the COI sequences were divided into 13 BINs in BOLD, and the sequences from the Fennoscandian specimens were divided into nine BINs. This correlates well with the concatenated ML tree where the sequences can be grouped into eight Fennoscandian clades and 12 clades in total. The ninth or thirteenth BIN was assigned to *S. rosenschoeldi*, dividing the species into two BINs.

The sequences are divided into the same clades for both the markers COI and AATSI. For the COI marker, GMYC delimits 11 clusters and 12 ML entities. The last entity is *S. akizukii*, which is only one specimen and could not be divided into a clade (Supplementary Figure A4). Eight of the clades are the Fennoscandian clades, and the other three are clades of specimens from outside of Fennoscandia. For the AATSI marker, GMYC delimits six clusters and eight ML entities (Supplementary Figure A5). The two ML entities that were not assigned a clade are the two sequences from the specimens *Stictochironomus* sp. 2TE. and *Stictochironomus* sp. *sticticus* Norway, meaning GMYC also assigned the AATSI sequences to the eight Fennoscandian clades. For the PGD marker, GMYC delimits only five clusters, and 14 ML entities. The high number of ML entities is largely caused by the *S. rosenschoeldi* sequences not being delimited into the same single clade, instead they are delimited into two separate clades and five additional ML entities. The two sequences of *S. psilopterus* and the two sequences of *Stictochironomus* sp. pi I were also not delimited into the same cluster. However, looking at the GMYC tree of the PGD sequences, the clades are delimited monophyletically into six of the Fennoscandian species (the sequences of *Stictochironomus* sp. *pictulus* II and *Stictochironomus* sp. *sticticus* Norway were removed from the PGD alignment and are therefore missing in the analysis) (Supplementary Figure A6).

Morphology

The morphological analysis show that there is a unique combination of diagnostic characters for all the previously described species, and for *Stictochironomus* sp. 2TE. For the two *S. pictulus* clades and the two *S. sticticus* clades, there were some morphological differences, but not enough to make a unique combination of diagnostic characters.

Stictochironomus maculipennis (Meigen, 1818)

Material examined: 3♂♂; 1♂, TRD-CH321, collected in Norway, Sør-Trøndelag, 63.429 10.379, 17.07.2014 by Stur, E.; 1♂, TRD-CH95, collected in Norway, Sør-Trøndelag, 63.425 10.282, 27.05.2014 Ekrem, T. et al., 1♂, ATNA568, collected in Norway, Hedemark, 61.74614 10.74618, 30.06.-07.07.2008 by Hoffstad, T.

Description

Size: body length 6.72-7.56 mm, wing length 3.43-3.82 mm, wing width 0.86-1.09 mm.

Coloration: Antenna brown. Head light brown. Flagellum brown. Maxillary light brown. Scutum color dark brown dorsal, light brown ventral. Scutellum brown, dark brown on edges. Postnotum dark brown to brown, lighter posteriorly ventral. Legs distinctly marked. Foreleg: femur dark brown with brown to light brown ring distally (sometimes absent) and fading to brown proximally; tibia brown to dark brown proximally and distally, middle brown to light brown with faint to distinct darker ring; tarsus I brown distally fading to light brown proximally (1/4 to 1/6) or dark brown distally (1/6), darker area around middle half and light brown proximally; tarsus 2-5 brown. Midleg: pattern like foreleg, but more distinct than both fore and midleg. Hindleg: pattern like foreleg but more distinct. Wing with distinct pattern: brownish spot around RM, grayish spots present around wing vein An, Cu₁, Cu₂, and M, in anal cell, and grayish pigmentation on the membrane along M, R₁, R₂₊₃ and R₄₊₅ and the rim of the wing near Cu₁. Abdominal tergites light brown with darker central line on tergite II-VI.

Head. Antennal ratio 2,187-2,474. Frontal tubercles absent. Temporals 18-20 (2). Palp 5-segmented. First to fifth segment lengths (µm): 46-60; 106-127; 181-203; 187-192; 239-276. Clypeus with 34-41 setae. Thorax. Acrostichals 2-4 (2). Dorsocentrals 16, originating from large pits, arranged in 1 row. Prealars 7-10. Supraalars absent. Scutellars 25-46. Wing. Squamals 22-34. Anal lobe well developed. R₂₊₃ running separately from both R₁ and R₄₊₅ and ending closer to R₁. FCu slightly proximal to RM. Cu₂ ending well proximal to the end of R₄₊₅. An ending almost on the rim of the wing. Legs. Fore tibia with an apical rounded scale bearing 2-3 strong setae. Middle and hind tibial combs fused with 1-2 spurs. Mid and hindleg bearded, hind leg strongest and longest setae. Leg segment lengths and proportions given in Supplementary Table B2 and B3. Hypopygium. Setae on tergite X 6-9. Hypopygium like Figure 7. Anal point long and straight. Gonocoxite long and narrow. Gonostylus long, about half the length of gonocoxite. Superior volsella almost straight with right angled hook apically to crescent shape with obtuse angled hook apically (Figure 15), with 5-6 basal setae and 1 short lateral seta. Inferior volsella slightly boomerang shaped (angled inwards), pubescent on entire surface with an apical long strong setae, and recurved strong setae.

1 female imago (ATNA569) and 1 larva (TRD-CHI13) known, but not measured.

Comments: *Stictochironomus maculipennis* is very similar to *S. pictulus* in coloration and patterns. However *S. maculipennis* has larger spots on the wings and slightly darker coloration on the wings and legs, and there is always a third band in the middle of fore tibia, whereas the third band is often absent in *S. pictulus*. The shape of superior volsella is also different (See Figure 14 and Figure 15).

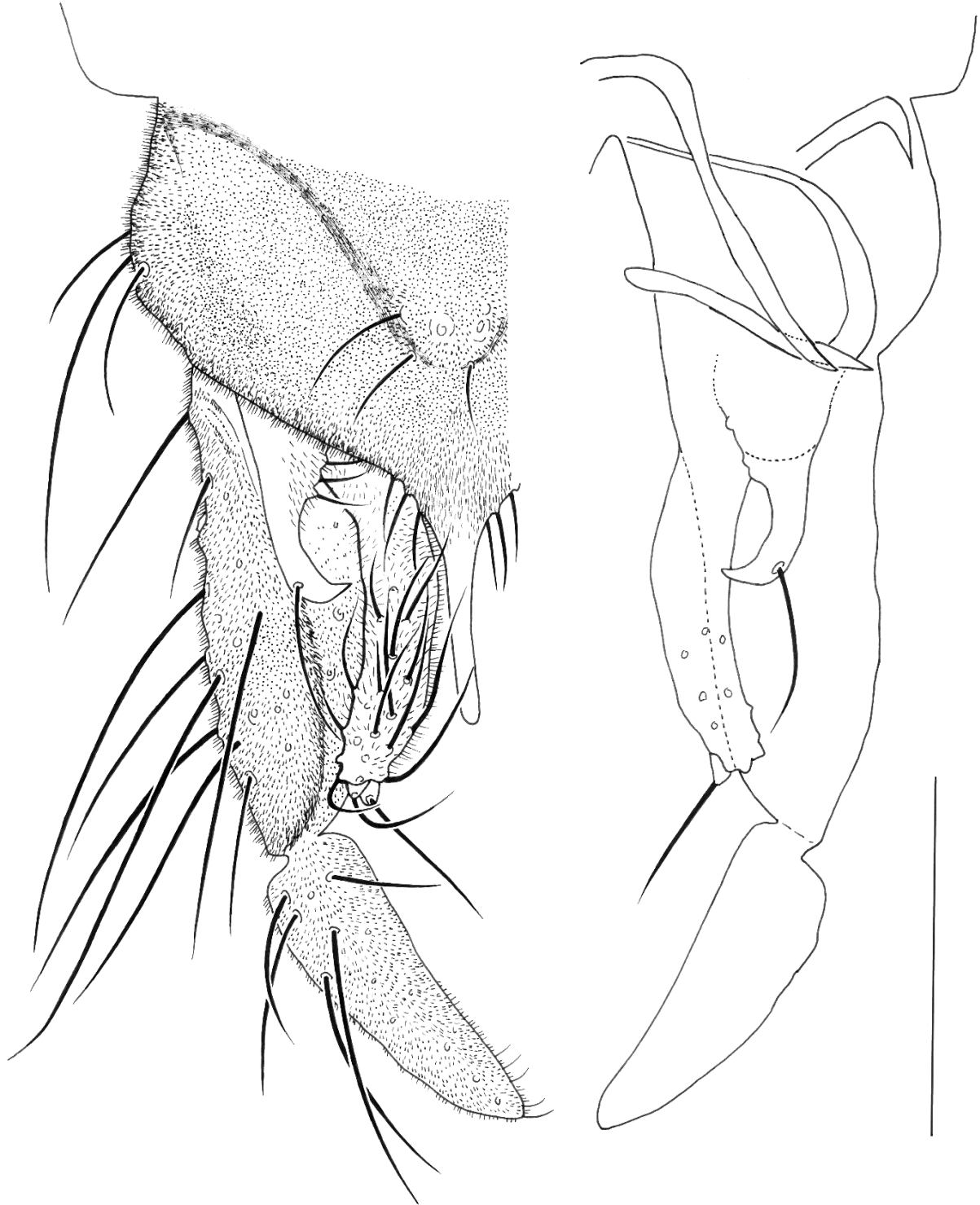


Figure 7 – Hypopygium of *Stictochironomus maculipennis*, the specimen depicted is BOLD specimen ID: TDR-CH95. Scalebar 200 μ m.

Stictochironomus sp. pictulus I

Material examined: 2♂♂, ZMUO.024720 and ZMUO.024721 collected in Finland, Varsinais-Suomi, 60.41 23.034, 17.05.2015 by Paasivirta, L.

Description

Size: body length 6.10-6.19 mm, wing length 2.80-2.93 mm, wing width not measurable.

Coloration: Antenna missing from both specimens. Head brown. Maxillary brown. Scutum color brown. Scutellum light brown. Postnotum brown. Legs distinctly marked. Foreleg: femur brown with light brown ring distally and proximal end light brown; tibia light brown and fading brown proximally and distally; tarsi brown. Midleg: pattern like foreleg, except tibia also has third brown ring in the middle. Hindleg: pattern like midleg but more distinct. Wing markings faint but clear. Brownish spot around RM. Grayish spots present in anal cell, m_{3+4} , and r_{4+5} , and around wing vein An, and grayish pigmentation on the membrane along wing vein M, R_1 and R_{2+3} . Abdominal tergites brown with slightly darker areas along the middle.

Head. Frontal tubercles absent. Temporals 16-18. Palp 5-segmented. First to fifth segment lengths (μm): 49-59; 77-82; 158 (1); 146-160; 199 (1). Clypeus with 23-26 setae. Thorax. Acrostichals 6-10. Dorsocentrals 12-13 originating from large pits, arranged in 1 row. Prealars 5. Supraalars absent. Scutellars 13-19. Wings. Squamals 20-22. Anal lobe well developed. R_{2+3} running separately from both R_1 and R_{4+5} and ending closer to R_1 . FCu slightly proximal to RM. Cu_2 ending well proximal to the end of R_{4+5} . An ending almost on the rim of the wing. Legs. Fore tibia with an apical rounded scale bearing 1-2 strong setae. Middle and hind tibial combs fused with 1-2 spurs. Mid and hind tibia and tarsi bearded, hind leg strongest and longest setae. Leg segment lengths and proportions given in Supplementary Table B2 and B3. Hypopygium. Setae on tergite X 4-8. Hypopygium like Figure 8. Anal point long and straight. Gonocoxite long and slightly peanut shaped. Gonostylus about half the length of gonocoxite. Superior volsella bulky with acutely angled hook, with 4 basal setae and 1 long lateral seta. Inferior volsella long and slightly bent outward, with 1 long seta apically, and recurved setae.

No larvae, pupa nor female imagines known or measured.

Comments: The two species that are perhaps the most difficult to tell apart are *Stictochironomus sp. pictulus I* and *Stictochironomus sp. pictulus II*. The diagnostic character that separate them is the number of setae on the thorax: *Stictochironomus sp. pictulus I* has around 12 dorsocentrals, 5 prealars, and 13-19 scutellars, whereas *Stictochironomus sp. pictulus II* has 20-26 dorsocentrals, 6 prealars and 34-37 scutellars. Furthermore, *Stictochironomus sp. pictulus I* is very similar to *S. maculipennis* in coloration and patterns. *Stictochironomus sp. pictulus I* has smaller spots on the wings and lighter coloration on the body, and the third band in the middle of the fore tibia is often absent. The shape of superior volsella is also different (See Figure 14 and Figure 15)

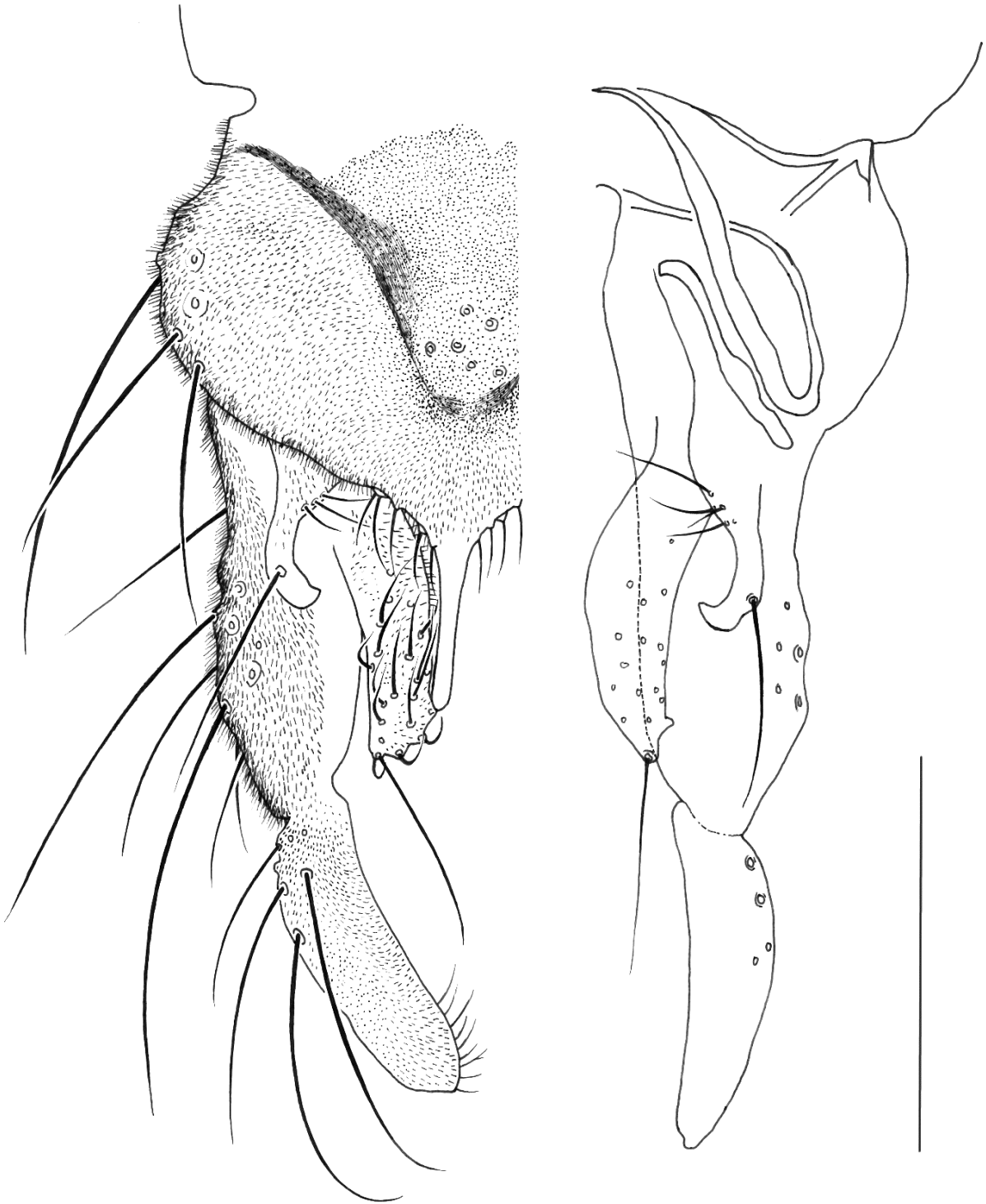


Figure 8 – Hypopygium of *Stictochironomus pictulus*, the specimen depicted is BOLD specimen ID: ZMUO.024720. Cluster *Stictochironomus* sp. *pictulus* I. Scalebar 200 μ m.

Stictochironomus sp. *pictulus* II

Material examined: 2♂♂, ZMUO.025172, ZUMO.025173 collected in Finland, , Satakunta 61.606 21.626 04.07.2015 by Paasivirta, L.

Description

Size: body length 7.21-7.80 mm, wing length 3.52-3.65 mm, wing width 0.82-0.90 mm.

Coloration: Antenna light brown. Head brown. Flagellum light brown. Maxillary brown. Scutum dark brown. Scutellum brown. Postnotum dark brown, lighter ventral posteriorly. Legs distinctly marked. Foreleg: proximal half of femur light brown to gradually brown, distal half dark brown with a light brown ring; 1/3 of proximal end and 1/6 of distal end of tibia dark brown, middle light brown with brown ring in the center, or middle ring absent; tarsus I light brown with brown area in middle and 1/10 of distal end dark brown; tarsi 2-5 brown. Midleg pattern similar to foreleg: femur brown to dark brown with light brown proximal end and light brown ring near distal end; tibia light brown with dark brown areas on both ends and middle; tarsi 1-2 light brown and dark brown distally; tarsi 3-5 brown. Hindleg pattern very similar to midleg, only with broader markings. Wing markings faint but clear. Brownish spot around RM. Grayish spots present in anal cell, m_{3+4} , and r_{4+5} , and around wing vein An, and grayish pigmentation on the membrane along wing vein M, R_1 and R_{2+3} . Abdominal tergites brown.

Head. Antennal ratio 2,358. Frontal tubercles absent. Temporals 20-22. Palp 5-segmented. First to fifth segment lengths (μm): 47-57; 108 (1); 186-194; 210 (1); 318 (1). Clypeus with 26-28 setae. Thorax. Acrostichals 13-17. Dorsocentrals 20-26 originating from large pits, arranged in 1 row. Prealars 8. Supraalars absent. Scutellars 34-37. Wings. Squamals 36-42. Anal lobe well developed. R_{2+3} running separately from both R_1 and R_{4+5} and ending closer to R_1 . FCu slightly proximal to RM. Cu_2 ending well proximal to the end of R_{4+5} . An ending almost on the rim of the wing. Legs. Fore tibia with an apical rounded scale bearing 1-3 strong setae. Middle and hind tibial combs fused with 1-2 spurs. Middle and hind legs bearded. Leg proportions given in Supplementary Table B2 and B3. Hypopygium. Setae on tergite X 5-6. Hypopygium like Figure 9. Anal point long and straight. Gonocoxite long and slender. Gonostylus slender and half the length of gonocoxite. Superior volsella shaped acutely angled like hook (Figure 14 C) and D)), with 4-5 basal setae and 1 medium long lateral seta. Inferior volsella slightly boomerang shaped with medium long distal seta, and medium long setae.

No larvae, pupa nor female imagines known or measured.

Comments: The two species that are perhaps the most difficult to tell apart are *Stictochironomus* sp. *pictulus* II and *Stictochironomus* sp. *pictulus* I. The diagnostic character that separate them is the number of setae on the thorax: *Stictochironomus* sp. *pictulus* II has 20-26 dorsocentrals, 6 prealars and 34-37 scutellars, whereas *Stictochironomus* sp. *pictulus* I has around 12 dorsocentrals, 5 prealars, and 13-19 scutellars. *Stictochironomus* sp. *pictulus* II is very similar to *S. maculipennis* in coloration

and patterns. *Stictochironomus* sp. *pictulus* II has smaller spots on the wings and lighter coloration on the body, and the third band in the middle of the fore tibia is often absent. The shape of superior volsella is also different (See Figure 14 and Figure 15).

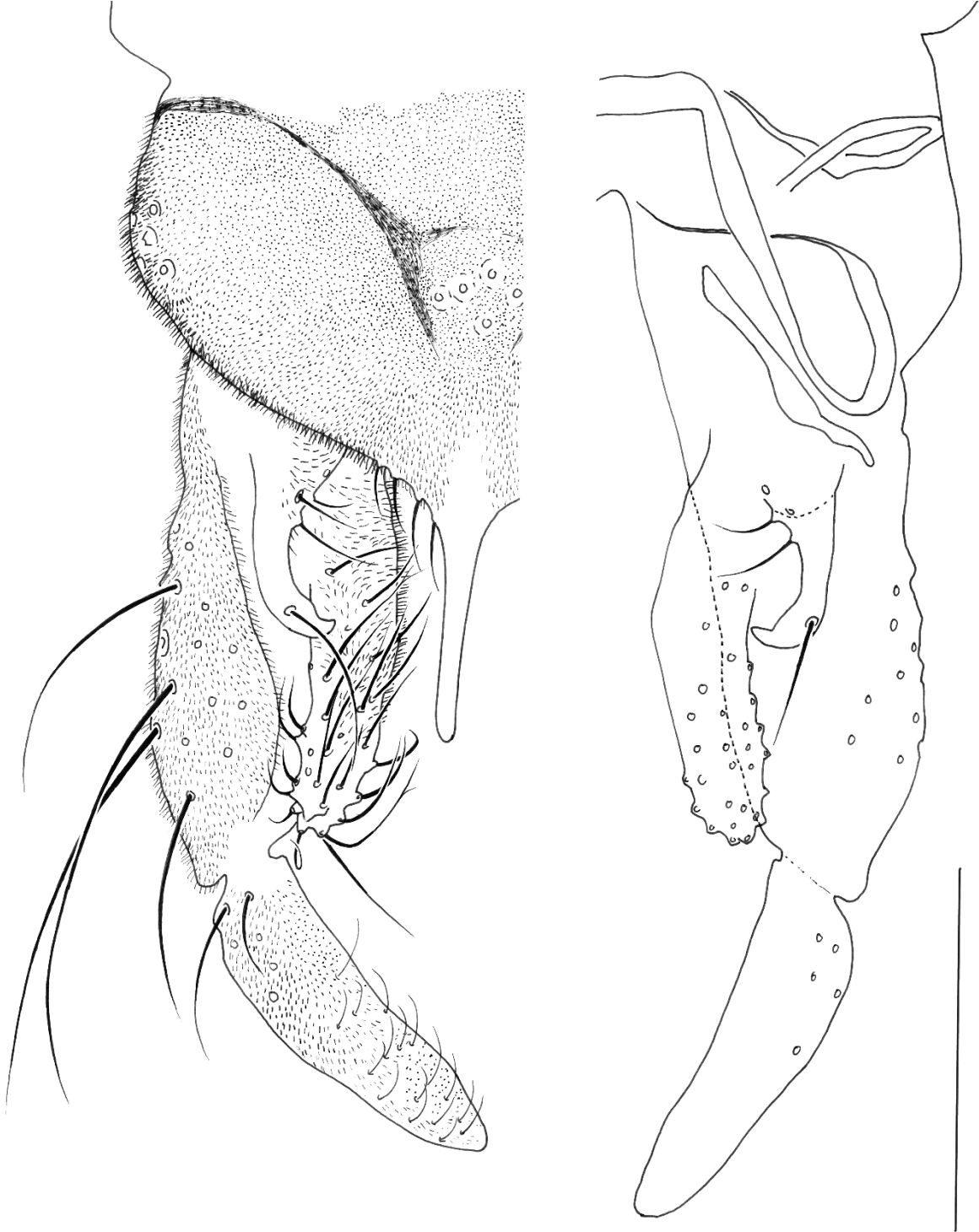


Figure 9 – Hypopygium of *Stictochironomus pictulus*, the specimen depicted is BOLD specimen ID: ZMUO.025173. Cluster *Stictochironomus* sp. *pictulus* II. Scalebar 200 μ m.

Stictochironomus psilopterus (Edwards, 1935)

Material examined: 2♂♂, BJ196, BJ198, collected in Norway, Bjørnøya, 74.47443 19.06310, 07.-20.07.2009 by Olsen, P. H., Finstad, A. G., Ekrem, T.

Description

Size: body length not possible to measure, wing length 4.55-4.94 mm, wing width 1.11 (1) mm.

Coloration: Antenna missing from both specimens. Head brown. Flagellum (MISSING). Maxillary light brown. Scutum color, dark brown. Scutellum dark brown. Postnotum dark brown. Legs dark brown. Wing with brownish spot around RM, veins An, Cu, Cu₁, Cu₂ and M₁₊₂ transparent, Sc, M, RM, R, R₁, R₂₊₃, R₄₊₅ pigmented brownish. Abdominal tergites brown to dark brown.

Head. Frontal tubercles absent. Temporals 20-25. Palp 5-segmented. First to fifth segment lengths (µm): 54-64; 90-95; 203-212; 215 (1); 276 (1). Clypeus with 47-57 setae. Thorax. Acrostichals 6(1). Dorsocentrals 31-36 originating from large pits, arranged in 2 rows posteriorly tapering to 1 row anteriorly. Prealars 12-16. Supraalars absent. Scutellars 64-66. Wings. Squamals 25-50. Anal lobe well developed. R₂₊₃ running separately from both R₁ and R₄₊₅ and ending closer to R₁. FCu about same level as RM. Cu₂ ending well proximal to the end of R₄₊₅. An ending almost on the rim of the wing. Legs. Fore tibia with an apical rounded scale bearing 1-3 strong setae. Middle and hind tibial combs fused with 1 spur. Middle legs, hind legs and fore femur bearded. Leg segment lengths and proportions given in Supplementary Table B2 and B3. Hypopygium. Setae on tergite X 8. Hypopygium like Figure 10. Anal point long and straight. Gonocoxite slightly peanut shaped. Gonostylus long and thinner apically. Superior volsella crescent shaped, evenly curved basally to apically, with 4-5 basal setae and 1 short lateral seta. Inferior volsella slightly bent, even thickness with recurved strong setae.

4 larvae known (BJ150, BJ218, BJ85, BJ98), but not measured.

Comments: *Stictochironomus psilopterus* is on overall appearance similar to *S. sticticus* and *Stictochironomus* sp. 2TE, however, the wings of *S. psilopterus* are unmistakable: the veins An, Cu, Cu₁, Cu₂ and M₁₊₂ are transparent, Sc, M, RM, R, R₁, R₂₊₃, R₄₊₅ are pigmented brownish.

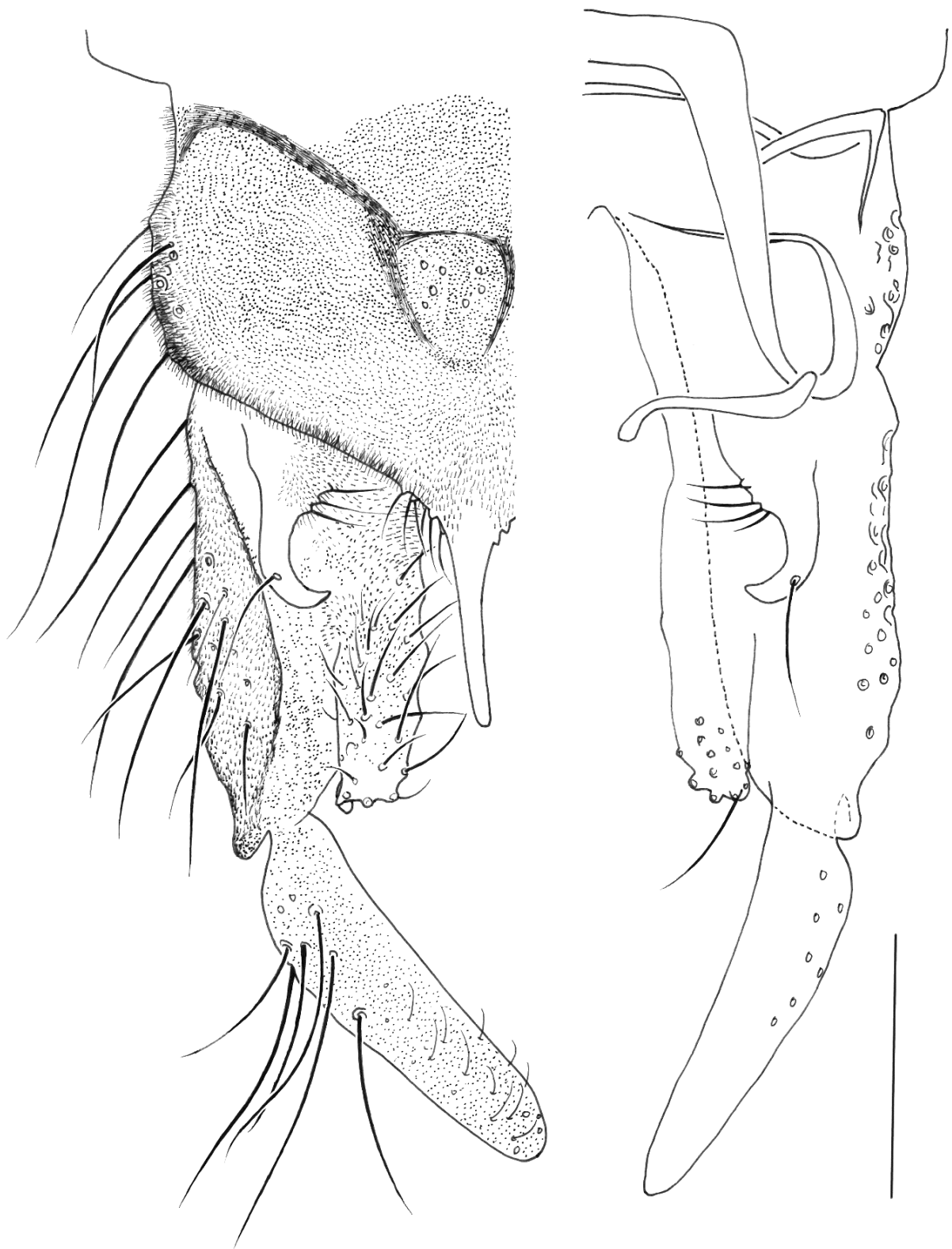


Figure 10 – Hypopygium of *Stictochironomus psilopterus*, the specimen depicted is BOLD specimen ID: BJ196. Scalebar 200 μm .

Stictochironomus rosenschoeldi (Zetterstedt, 1838)

Designated lectotype: *C. assimilis*, Zett. collected in Lycksele, Sweden. 1990. Specimen number 7. MZLU 00182197.

Material examined: 9♂♂; 1♂, Finnmark527, collected in Norway, Finnmark, 70.45214 27.01012, 17.06.2010, collected by Ekrem, T. & Stur, E.; 1♂, Finnmark653, collected in Norway, Finnmark, 70.44099 26.80499, 17.06.2010 by Ekrem, T. & Stur, E.; 2♂, ZMUO.024303 and ZUMO.024304 collected in Finland, Varsinais-Suomi, 60.314 23.29, 28.06.2015 by Paasivirta, L.; 2♂, ZMUO.024596 and ZUMO. 024597, collected in Finland, Varsinais-Suomi, 61.07 25.055, 09.05.2015 by Paasivirta, L.; 2♂, NORIR01 and NORIR04, collected in Norway, Sør-Trøndelag, 63.24068 10,436460, 18.05.2022 by Ekrem, T. & Stur, E.; 1♂, NORIR10 collected in Norway, Finnmark, 70.13477 29,011310, 11.06.2022 by Reistad, I.

Description

Size: body length 5.35-6.39 mm, wing length 2.61-3.12 mm, wing width 0.65-0.69 mm.

Coloration: Antenna. Head dark brown. Flagellum brown. Maxillary brown. Scutum dark brown. Scutellum brown. Postnotum dark brown. Legs brown. Wing with brownish spot on membrane surrounding RM, sometimes absent and brownish pigmentation on wing veins, often milky pigmentation on whole membrane. Abdominal tergites brown.

Morphology: Head. Antennal ratio 2,389-2,55 (6). Frontal tubercles absent. Temporals 12-20. Palp 5-segmented. First to fifth segment lengths (µm): 39-61; 76-106; 155-184 (6); 141-184 (7); 173-237 (5). Clypeus with 21-33 setae. Thorax. Acrostichals 6-12. Dorsocentrals 17-26 originating from large pits, arranged in 1-2 rows, or 1 row sometimes with two setae side by side. Prealars 6-10. Supraalars absent. Scutellars 23-29. Wing. Squamals 8-31. Anal lobe well developed. R₂₊₃ running separately from both R₁ and R₄₊₅ and ending closer to R₁. FCu about same level as RM. Cu₂ ending well proximal to the end of R₄₊₅. An ending almost on the rim of the wing. Legs Fore tibia with an apical rounded scale bearing 3 strong setae. Middle and hind tibial combs fused with 1-2 spurs. Mid and hind legs and fore femur bearded. Leg segment lengths and proportions given in Supplementary Table B2 and B3. Hypopygium. Setae on tergite X 5-14. Hypopygium like Figure 11. Anal point long and straight. Gonocoxite long and slender. Gonostylus about half the length of gonocoxite. Superior volsella almost straight and thickest around the midpoint, with 3-6 basal setae and 1 long lateral seta. Inferior volsella long and slightly bent, with an apical long seta, and recurved setae.

No larvae, pupa nor female imagines known or measured.

Comments: *Stictochironomus rosenschoeldi* is not easily confused with the other species. It is smaller than all the other species, the total body length of 5.86 mm is on average 0.6 mm shorter than the next smallest species that look similar morphologically (*Stictochironomus* sp. 2TE). The wings of *S. rosenschoeldi* often has a milky color, which has not commonly been observed in the other Fennoscandian species. The superior

volsella are almost straight, while the other species mostly have hook or crescent shaped superior volsella.

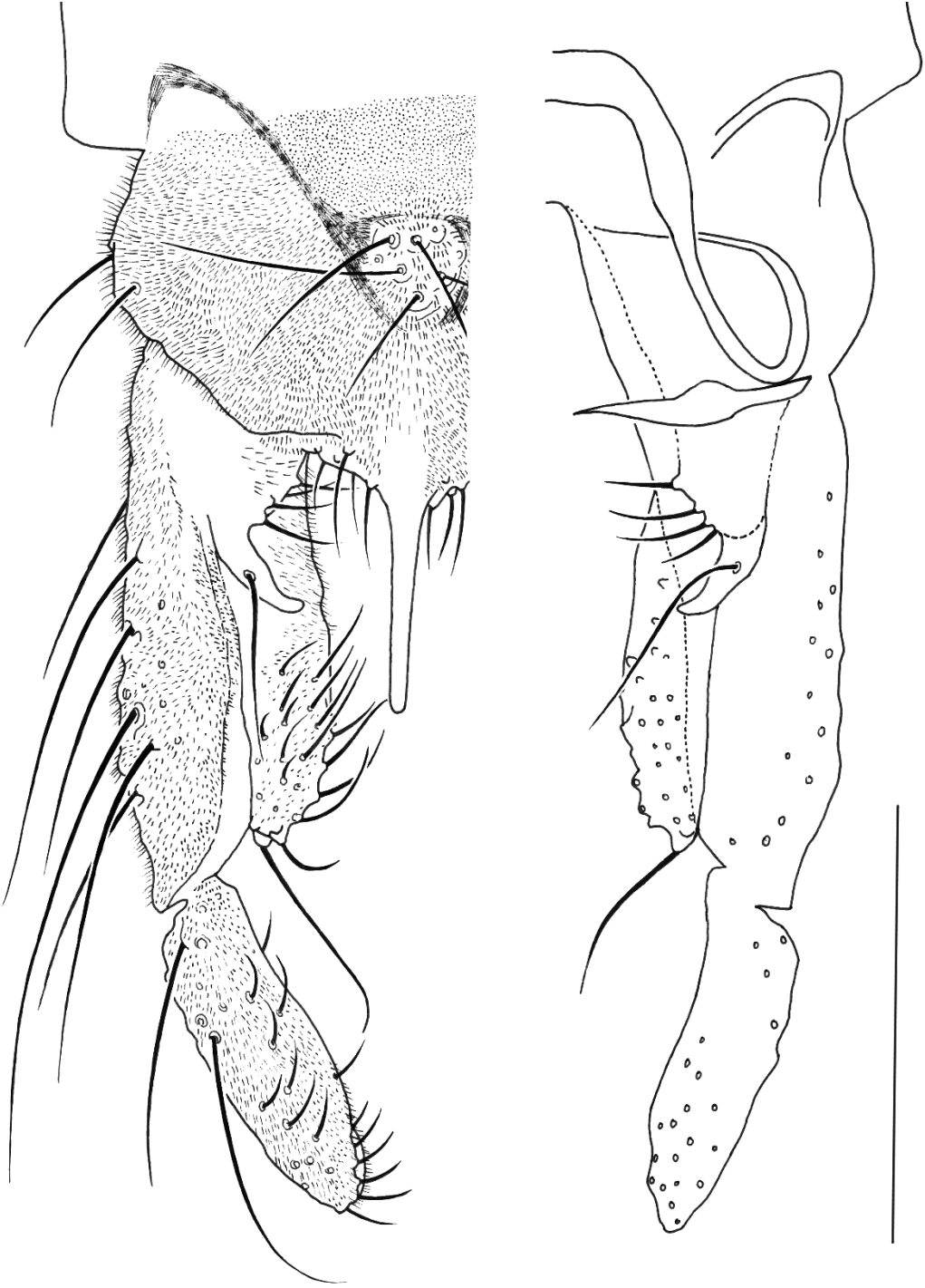


Figure II - Hypopygium of *Stictochironomus rosenschoeldi*, the specimen depicted is BOLD specimen ID: Finnmark527. Scalebar 200 μ m.

Stictochironomus sp. 2TE

Material examined: 2♂♂; 1♂, Finnmark108, collected in Norway, Finnmark, 70.32152 31.03407, 18.06.2010 by Ekrem, T. & Stur, E.; 1♂, Finnmark385, collected in Norway, Finnmark, 69.84383 26.07607, 16.06.2010 by Ekrem, T. & Stur, E.

Diagnosis

Size: body length 6.43 (1) mm, wing length 3.39-3.67 mm, wing width 0.89-0.87 mm.

Coloration: Antenna brown. Head brown. Flagellum dark brown. Maxillary palp brown/light brown. Scutum brown. Scutellum light brown. Postnotum brown. Legs brown with light brown ring between trochanter and femur. Wing with brownish spot on membrane surrounding RM and brownish pigmentation on Sc, R, R₁, R₂₊₃, R₄₊₅ and M, while vein An, Cu, Cu₁, Cu₂ and M₁₊₂ are almost transparent. Abdominal tergites light brown with darker central line on tergite II-VI.

Morphology: Head. Antennal ratio 3.01-3.65. Frontal tubercles absent. Temporals 15-18. Palp 5-segmented. First to fifth segment lengths (µm): 59-65; 103-108; 203-229; 194-195; 257-292. Clypeus with 30-32 setae. Thorax. Acrostichals 8. Dorsocentrals 42-43 (43), originating from large pits, arranged in three rows posteriorly tapering to two rows anteriorly. Prealars 19-20. Supraalars absent. Scutellars 59 (1). Wing. Squamals 30-40. Anal lobe well developed. R₂₊₃ running separately from both R₁ and R₄₊₅ and ending closer to R₁. FCu about same level as RM. Cu₂ ending well proximal to the end of R₄₊₅. An ending almost on the rim of the wing. Wings. Fore tibia with an apical rounded scale bearing 1-2 strong setae. Middle and hind tibial combs fused with 1 spur. Mid and hind legs bearded, fore femur bearded, hind leg strongest and longest setae. Leg segment lengths and proportions given in Supplementary Table B2 and B3. Hypopygium. Setae on tergite X 12-15. Hypopygium like Figure 12. Anal point long and straight. Gonocoxite long and narrow. Gonostylus long, about half the length of gonocoxite with very fine microtrichia. Superior volsella long and curved, blunt apically, with 5-8 (7) basal setae and 1-2 short lateral setae. Inferior volsella almost straight and narrowing apically, pubescent on entire surface with an apical long strong setae that is sometimes clefted, and strong recurved setae.

Pupa known by two individuals (Finnmark781, Finnmark782), but not measured.

Differential diagnosis: The species is morphologically most similar to *S. sticticus* (Fabricius, 1781) in coloration, wing pattern, and the general shape of the hypopygium. However, *Stictochironomus* sp. 2TE has over 40 dorsocentrals arranged in 2-3 rows, whereas *S. sticticus* has 18-30 dorsocentrals arranged in 1-2 rows. In addition, the gonostylus and gonocoxite of *Stictochironomus* sp. 2TE is slenderer, and the superior volsella is blunter apically.

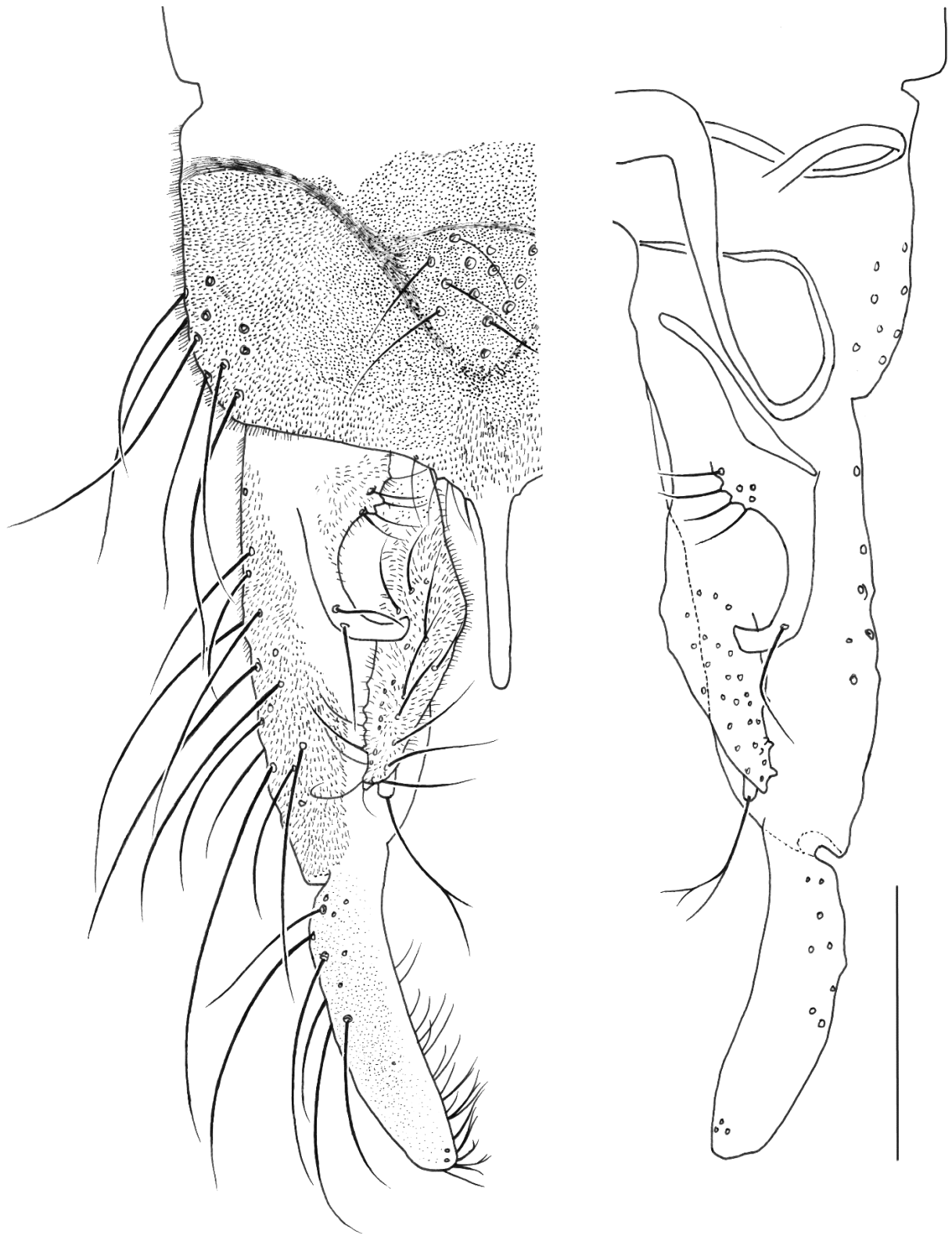


Figure 12 – Hypopygium of *Stictochironomus* sp. 2TE, the specimen depicted is BOLD specimen ID: Filnmark108. Scalebar 200 μ m.

Stictochironomus sp. *sticticus* Norway

Material examined: 2♂♂; 1♂, Finnmark202, collected in Norway, Finnmark, 69.8306 25.1856, 03.09.2010 by Andersen, A.; 1♂, TRD-CH281, collected in Norway, Sør-Trøndelag, 63.27444 10.56131, 14.-28.08.2014 by Stur, E. et al.

Description

Size: body length 7.08-7.32 mm, wing length 3.67-3.69 mm, wing width 0.98-0.92 mm.

Coloration: Antenna brown. Head dark brown. Flagellum brown. Maxillary dark brown. Scutum dark brown. Scutellum dark brown. Postnotum dark brown. Legs dark brown. Wing with brownish spot on membrane surrounding RM and brownish pigmentation on wing veins. Abdominal tergites brown with darker line down center.

Morphology: Head. Antennal ratio 2,579-2,882. Frontal tubercles absent. Temporals 17-23. Palp 5-segmented. First to fifth segment lengths (µm): 66-70; 89-98; 181-191; 191-202; 308 (1). Clypeus with 15-18 setae. Thorax. Acrostichals 4-6. Dorsocentrals 18-26 originating from large pits, arranged in 1 row, with some setae side by side. Prealars 8-9. Supraalars absent. Scutellars 34-40. Wings. Squamals 16-22. Anal lobe well developed. R₂₊₃ running separately from both R₁ and R₄₊₅ and ending closer to R₁. FCu about same level as RM. Cu₂ ending well proximal to the end of R₄₊₅. An ending almost on the rim of the wing. Legs. Fore tibia with an apical rounded scale bearing 2 strong setae. Middle and hind tibial combs fused with 1-2 spurs. Mid and hind legs and fore femur bearded. Leg segment lengths and proportions given in Supplementary Table B2 and B3. Hypopygium. Setae on tergite X 6. Hypopygium like Figure 13. Anal point long and straight. Gonocoxite long and straight. Gonostylus long and rounded, about half the length of gonocoxite. Superior volsella hook to crescent shape with a sharp point apically, with 6 basal setae and 1 long lateral seta. Inferior volsella long and straight with an apical long setae and recurved setae.

1♂ known (To49), but not measured.

Comments: *Stictochironomus* sp. *sticticus* Norway can be confused with *Stictochironomus* sp. 2TE, as they are quite similar overall. They can easily be separated by looking at setae on the thorax: *Stictochironomus* sp. *sticticus* Norway has 18-26 dorsocentrals arranged mostly in one row, 8 prealars and 34-40 scutellars, whereas *Stictochironomus* sp. 2TE has more than 40 dorsocentrals arranged in three rows, 20 prealars and about 60 scutellars. *Stictochironomus* sp. *sticticus* Norway is morphologically indistinguishable from *Stictochironomus* sp. 3TE, except that some specimens of *Stictochironomus* sp. 3TE has a faint pattern on the legs and *Stictochironomus* sp. *sticticus* Norway do not.

Stictochironomus sp. 3TE

Material examined: 5♂♂; 2♂, ZMUO.024315 and ZMUO.024316, collected in Finland, Varsinais-Suomi, 60.243 24.021, 01.05.2015 by Paasivirta, L.; 2♂, ZMUO.024599 and ZMUO.024598, collected in Finland, Varsinais-Suomi, 61.07 25.055, 09.05.2015 by Paasivirta, L.; 1♂, Finnmark 51, collected in Norway, Finnmark 69.21029 23.76200, 12.06.2010 by Ekrem, T. & Stur, E.

Size: body length 7.52-8.22 mm, wing length 3.62-3.95 mm, wing width 0.88-1.03 mm.

Coloration: Antenna brown. Head dark brown. Flagellum brown. Maxillary brown. Scutum dark brown. Scutellum dark brown. Postnotum dark brown. Legs faint markings. Foreleg: femur light brown on proximal end, otherwise dark brown. Midleg: femur dark brown; tibia dark brown with two brown bands; tarsi brown. Hindleg: markings like foreleg. Wing with brownish spot on membrane surrounding RM and brownish pigmentation on wing veins. Abdominal tergites brown with dark brown stripe down middle (very distinct).

Morphology: Head. Antennal ratio 3,449 (1). Frontal tubercles absent. Temporals 23. Palp 5-segmented. First to fifth segment lengths (µm): 58-64; 81-102; 152-201 (4); 21-203; 190-293 (4). Clypeus with 24-47 setae. Thorax. Acrostichals not able to count. Dorsocentrals 18-30 originating from large pits, arranged in 1 row, sometimes with two setae side by side. Prealars 10-15. Supraalars absent. Scutellars 40-53. Wing. Squamals 23-40. Anal lobe well developed. R₂₊₃ running separately from both R₁ and R₄₊₅ and ending closer to R₁. FCu about same level as RM. Cu₂ ending well proximal to the end of R₄₊₅. An ending almost on the rim of the wing. Legs. Fore tibia with an apical rounded scale bearing 3 strong setae. Middle and hind tibial combs fused with 1-2 spurs. Mid and hind legs bearded. Leg segment lengths and proportions given in Supplementary Table B2 and B3. Hypopygium. Hypopygium. Setae on tergite X 3-7. Hypopygium like Figure 13. Anal point long and straight. Gonocoxite long and robust. Gonostylus long and robust, about half the length of gonocoxite. Superior volsella hook to crescent shape with a sharp point apically, with 4-8 basal setae and 1 long lateral seta. Inferior volsella slightly bent, with an apical seta slightly longer than the other recurved setae.

No larvae, pupa nor female imagines known or measured.

Comments: *Stictochironomus* sp. 3TE can be confused with *Stictochironomus* sp. 2TE, as they are quite similar overall. They can easily be separated by looking at setae on the thorax: *Stictochironomus* sp. *sticticus* Norway has 18-30 dorsocentrals arranged mostly in one row, 10-15 prealars and 40-53 scutellars, whereas *Stictochironomus* sp. 2TE has more than 40 dorsocentrals arranged in three rows, 20 prealars and about 60 scutellars. *Stictochironomus* sp. *sticticus* Norway is morphologically indistinguishable from *Stictochironomus* sp. 3TE, except that some specimens of *Stictochironomus* sp. 3TE has a faint pattern on the legs and *Stictochironomus* sp. *sticticus* Norway do not.

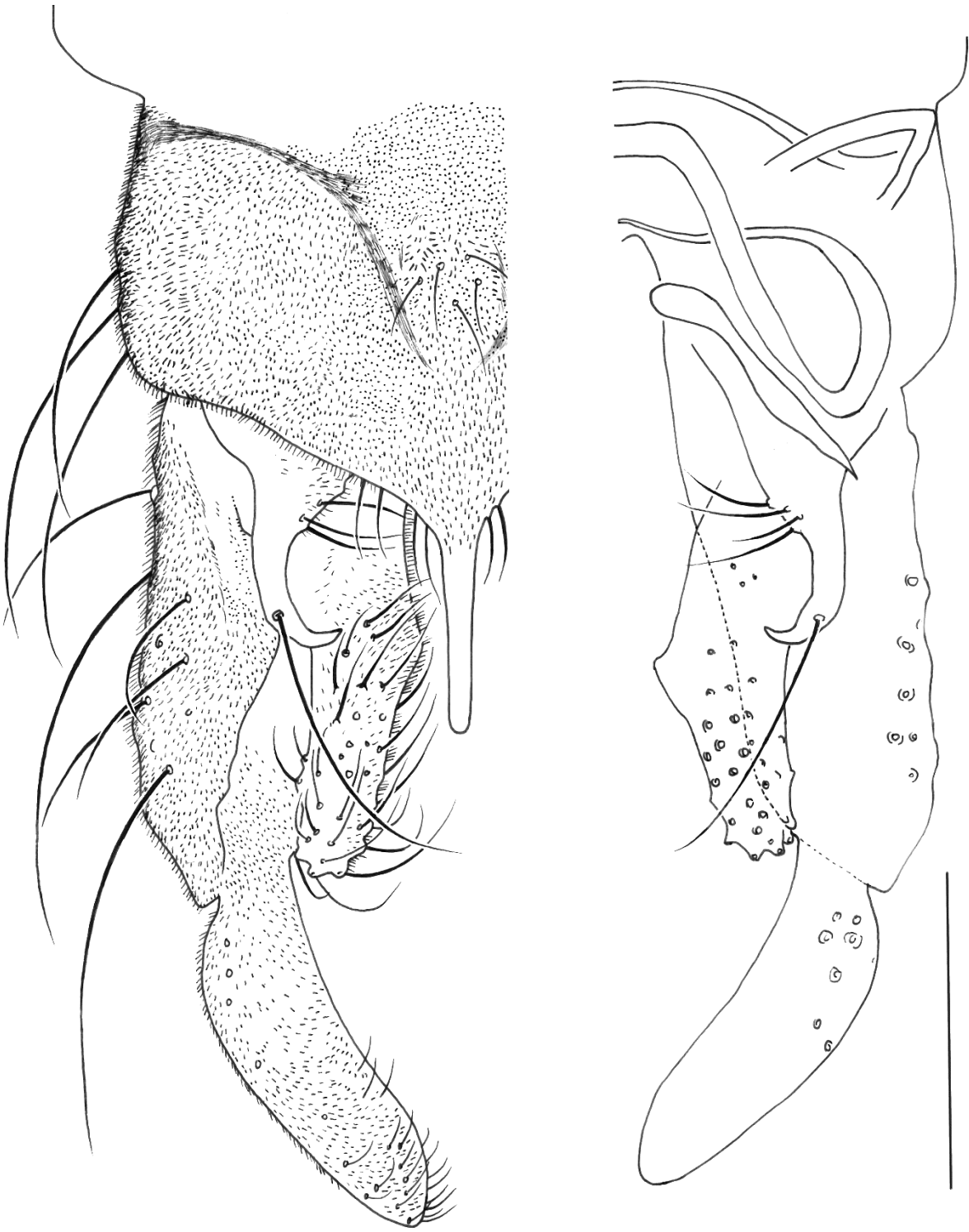


Figure B – Hypopygium of *Stictochironomus* sp. 3TE, the specimen depicted is BOLD specimen ID: ZMUO.024598. Scalebar 200 μ m.

Other species

Stictochironomus labeculatus (Goethghebuer 1938:58) has been classified as a nomen dubium. Coloration. Thorax and head brown. Wings have spot on membrane surrounding RM, veins Sc, M, RM, R, R₁, R₂₊₃, R₄₊₅ pigmented brownish, veins An, Cu, Cu₁, Cu₂ and M₁₊₂ faintly pigmented. Legs distinct pattern. Fore leg: femur brown 1/8 distally. Tibia brown 2/5 proximally and 1/8 distally. Tarsus 1 fading to brown distally. Tarsi 2-5 brown. Mid leg: light brownish yellow. Femur brown 1/8 distally, tibia brown 1/8 proximally and 1/8 distally, tarsus 1 brown 1/6 distally, tarsus 2-5 brown. Hind leg: femur 1/8 brown distally, tibia brown 1/6 proximally and brown 1/8 distally, tarsus 1 brown 1/6 distally, tarsus 2-3 fading to brown distally, tarsus 4-5 brown. Morphology. Head 18 temporals. Thorax. Acrostichals 8. Dorsocentrals 18-23. Hypopygium. Setae on tergite X 8. Superior volsella slender and almost straight with a little nub apically.

Stictochironomus stackelbergi (Goethghebuer, 1938: 56) has been classified as a nomen dubium. Coloration. Thorax, head and legs light brown. Wings have spot on membrane surrounding RM. Morphology. Head 12-19 temporals. Thorax. Dorsocentrals 11, arranged in 1 row. Prealars 5. Hypopygium. Setae on tergite X 3. Superior volsella slender and hook shaped.

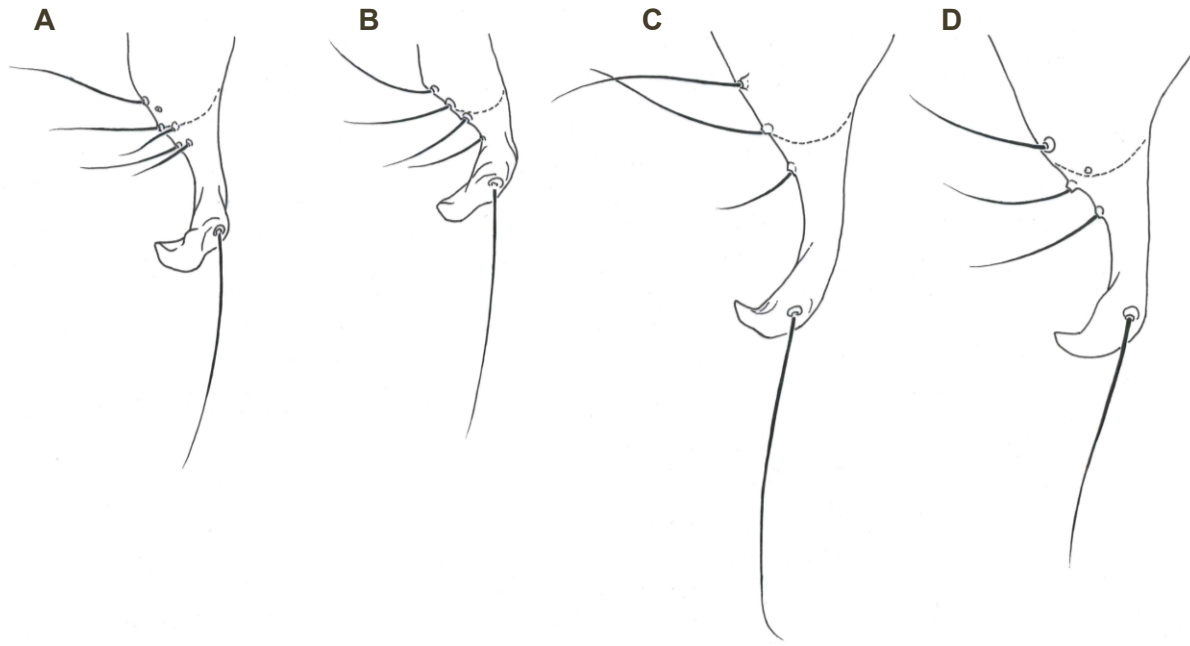


Figure 14 – Illustrations showing variance of superior volsella in *S. pictulus*. Specimens A) BOLD specimen ID: ZUMO.024720 and B) BOLD specimen ID: ZUMO.024721 fall within the cluster *Stictochironomus* sp. *pictulus* I and specimens C) BOLD specimen ID: ZUMO.025172 and D) BOLD specimen ID: ZUMO.025173 fall within the cluster *Stictochironomus* sp. *pictulus* II. For size see figure of hypopygium.

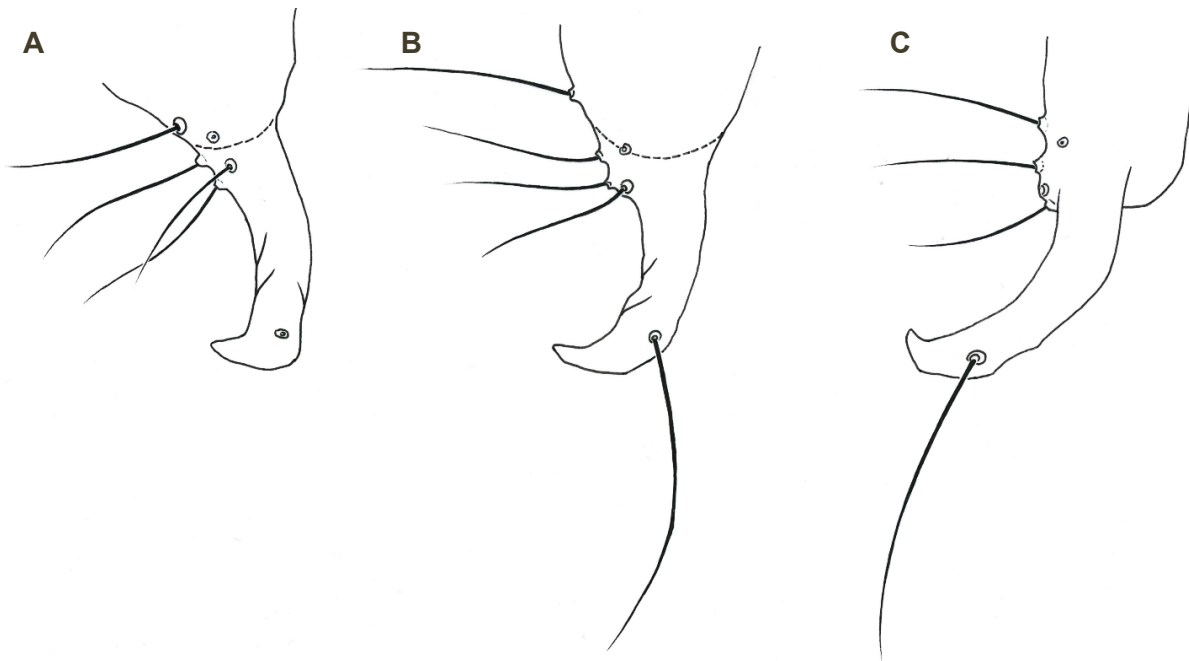


Figure 15 – Illustrations showing variance of superior volsella in *S. maculipennis*. Specimens A) BOLD specimen ID: AT568, B) BOLD specimen ID: TRD-CH95, C) BOLD specimen ID: TRD-CH321. For size see figure of hypopygium.

Key to male adults of the Fennoscandian *Stictochironomus* species

The characters for *S. crassiforceps* are written as according to Cranston et al. (1989). Point 2 in the key is largely adapted from Pinder (1978), otherwise I have observed and measured all the characters myself.

- 1 Inferior volsella short and medially curved, median anal tergite setae absent, reduced antenna ***Stictochironomus crassiforceps***
- Inferior volsella long and slender, median anal tergite setae present, antennae fully plumose. **2**
- 2 Wing membrane has several greyish spots around the apical end of veins and one brownish spot around RM **3**
- A single brownish spot is present around RM, or else RM and adjacent veins pigmented brownish, and wing otherwise unmarked **5**
- 3 Wing markings distinct. Grayish spots present around wing vein An, Cu₁, Cu₂, and M, in anal cell, and grayish pigmentation on the membrane along M, R₁, R₂₊₃ and R₄₊₅ and the rim of the wing near Cu₁. Leg markings brownish to yellowish to sometimes light, always with third band in the middle of fore tibia. Superior volsella almost straight with right angled hook apically to crescent shape with obtuse angled hook apically (Figure 15). Hypopygium in Figure 7 ***S. maculipennis***
- Wing markings faint but clear. Grayish spots present in anal cell, m₃₊₄, and r₄₊₅, and around wing vein An, and grayish pigmentation on the membrane along wing vein M, R₁ and R₂₊₃. Leg markings distinct brownish to light, third band in the middle of fore tibia often absent. Superior volsella crescent shape with acute angled hook apically or very bulky crescent shape (Figure 14) **4**
- 4 Thorax with 12-13 dorsocentrals, 5 prealars and 13-19 scutellars. Wing vein R with 19-21 setae, R₁ with about 10 setae and squama with 20-22 setae. Superior volsella like Figure 14 A and B. Hypopygium in Figure 8 ***Stictochironomus sp. pictulus I***
- Thorax with 20-26 dorsocentrals, 8 prealars and 34-37 scutellars. Wing vein R with 26-30 setae, R₁ with 16-25 setae and squama with 36-40 setae. Superior volsella like Figure 14 C and D. Hypopygium in Figure 9 ***Stictochironomus sp. pictulus II***
- 5 Wing veins An, Cu, Cu₁, Cu₂ and M₁₊₂ transparent and hard to see. Wing vein Sc, M, RM, R, R₁, R₂₊₃, R₄₊₅ pigmented brownish. Hypopygium in Figure 10 ***S. psilopterus***
- All wing veins pigmented brownish **6**
- 6 Superior volsella almost straight, with obtuse angled hook. Wing membrane often milky white. Cross-vein RM and neighboring veins brownish, brownish on membrane around RM sometimes absent. Hypopygium in Figure 11 ***S. rosenschoeldi***

- Superior volsella with acute angled hook. Wing membrane clear. Brownish spot on RM and surrounding membrane 7
- 7 Thorax has 18-30 dorsocentrals in 2 rows tapering to 1 posteriorly, and 8-15 prealars. Hypopygium in Figure 13 *S. sticticus*
- Thorax has more than 40 dorsocentrals in 3 rows tapering to 2 posteriorly, and ca. 20 prealars. Hypopygium in Figure 12 *Stictochironomus* sp. 2TE

Discussion

Phylogenetic trees

This study was initiated since available barcodes within the genus in BOLD showed larger divergence between putative species than was currently known from Fennoscandia. My phylogenetic analyses using the protein coding nuclear markers PGD and AATSI resulted in the same groups as seen in the phylogeny using COI-barcodes: there are eight genetic clusters of *Stictochironomus* in Fennoscandia. The purpose of the phylogenetic analyses in this study was to examine species boundaries within the genus. Thus, while the concatenated ML tree has many well supported branches in the lower parts of the tree, the limited taxonomic sampling makes the result not trustworthy as a proper reconstruction of the phylogenetic relationships between species in *Stictochironomus*. With regard to species delimitation, three new species are genetically distinct from each other and from the previously described species. Results from the concatenated ML tree (Figure 5) show that the two *S. pictulus* clades are not sister taxa, and neither are the two *S. sticticus* clades, even though morphologically adult males of these two species pair are the most similar to each other within the genus.

Some of the specimens were already barcoded and mounted on microscope slides (marked in white and dark green in Supplementary Table B1), and it was therefore not possible to extract DNA for molecular analysis of the genetic markers PGD. And AATSI. The new species *Stictochironomus* sp. 2TE and the potential new species *Stictochironomus* sp. *sticticus* Norway was thus only represented with one sequence in the phylogeny of AATSI, but the since the PGD sequences was of too low quality, these species were not represented in the phylogeny of PGD. Inclusion of more sequences from these two species could have revealed a different topology in the concatenated tree than what was revealed with the limited number of sequences from the nuclear markers. The fourth marker, CAD1 have been used successfully in previous studies of chironomids (Lin et al., 2018), but did not work very well on *Stictochironomus*. There are many steps in the extraction and amplification of DNA, and a lot could go wrong. To get better quality sequences it might be worth manipulating the PCR steps to make PGD work better, or test other markers, such as CAD4. In the AATSI tree, the two clades are not

sister taxa, but still closely related. With only two sequences included outside of COI, the clades have not been supported by more molecular evidence.

Another species that was not included in any of the phylogenetic analyses was *S. crassiforceps*. *Stictochironomus crassiforceps* has been recorded in Sweden and Finland historically, and could possibly exist in Norway as well. According to GBIF (2022) there are eight occurrences in Finland after 2003, but these specimens were only observed and not preserved. There are five preserved specimens from Russia, but I do not have access to the specimens or any photographs of the specimens. There are no recent recordings of *S. crassiforceps* in Sweden or Norway. I do not have access to any barcoded sequences through BOLD and could therefore not include it in the phylogenetic analyses. As this study aimed to review all the species of *Stictochironomus* in Fennoscandia, it would have been optimal to include *S. crassiforceps* as well. Since all the other species form well supported clades, it is unlikely that *S. crassiforceps* would affect the whole phylogeny in a way that changes the delimitation of the other species. It would be interesting to see if all specimens of *S. crassiforceps* would be assigned to the same clade, or if it would be divided into several clades like the *S. pictulus* and *S. sticticus* species. Including *S. crassiforceps* in the study could have revealed even more hidden diversity within the genus.

Similar studies have been done on other genera within Chironominae where seemingly identical morphological species showed great genetic variation. After studying the morphology thoroughly, a unique combination of diagnostic characters were revealed and the new species could be described and named (Anderson et al., 2013). Molecular analysis of COI is an effective way to reveal hidden species diversity in morphologically similar species. However, species specific genetic markers can with benefit be applied in the analysis to solidify the results.

Delimitation - GMYC

The GMYC result from the COI and AATSI markers show the same delimitation as the concatenated ML tree, that there are eight species of *Stictochironomus* in Fennoscandia. The shape of the line-through-time plot (Supplementary Figure A4 and A5) indicate that the separation between intraspecific and interspecific branching evens with a steep increase and towards the end. The red line shows where the separation was set (Song et al., 2018). In many studies, GMYC tends to oversplit species (Pentinsaari et al., 2017; Tänzler et al., 2012), but in this case the GMYC analysis divided the sequences into the same clusters as the phylogenetic analysis.

For the PGD marker, the results from the GMYC were not as clear. The shape of the PGD line-through-time plot (Supplementary Figure A6) is almost linear, meaning the GMYC analysis could not separate between interspecific and intraspecific branching events. Despite PGD having the longest sequence lengths, it has the least variation between base pairs of all the markers. Some of the sequences were also overall of worse quality than

the AATSI and COI sequences. This could have played a part in why so few clades were delimited.

Morphology

The species that have been described previously are all well established and have a unique combination of diagnostic characters. These species include *S. maculipennis*, *S. psilopterus* and *S. rosenschoeldi*. Characters that proved the most useful for distinguishing the new species were number setae on the thorax (dorsocentrals, prealars and scutellars), and the shape of the hypopygium and superior volsella.

The new species *Stictochironomus* sp. 2TE (sp. 2TE) also have a unique combination of diagnostic characters. The number of dorsocentrals is over 42-43, which is much higher than in the other species. Only *S. psilopterus* comes close with a maximum number of 36 dorsocentrals. In addition, the arrangement of dorsocentrals in sp. 2TE is unique in that they form three lines, tapering to two lines anteriorly. The number of prealars is higher than the other species; sp. 2TE has an average of 19,5 and the next species in line is *S. psilopterus* which has 14 prealars on average. *S. psilopterus* has more scutellars than sp. 2TE, 65 and 59 respectively. In short, the thorax of sp. 2TE is much hairier than the rest of the species, except for *S. psilopterus*. These two species can easily be separated by looking at the pigmentation on the wing veins. The number of setae on the tergite X is 13,5 which is about twice that of the other species. Some of the setae on the hypopygium are clefted. However, only one of the specimens have this trait, and it appear irregularly in other species as well. This trait exist more widely in other genera within Chironomini (Cranston et al., 1989), and it does not appear to be a good diagnostic character.

Even though I did not have access to any specimens of *S. crassiforceps* and could only refer to descriptions in literature and a drawing of its hypopygium, it is enough to conclude that none of the new species is a *S. crassiforceps*. The hypopygium of *S. crassiforceps* is unmistakable (Cranston et al., 1989). The illustration of hypopygium from the type specimen (Goetghebuer, 1932) seems to be the same as in (Cranston et al., 1989). No literature does, however, describe *S. crassiforceps* in great detail. Kieffer (1922) described the wing as being “finely dotted”. Solely based on this literature, it is not possible to know if the wing of *S. crassiforceps* looks more like the wing of *S. maculipennis* and *S. sticticus*, or if it only has the single spot on RM.

All the potential new species were compared morphologically to specimens of the two nomina dubia *Stictochironomus labeculatus* (Goetghebuer, 1938) and *S. stackelbergi* (Goetghebuer, 1938). The combination of characters on these two species are unique and not similar to the *Stictochironomus* species found in Fennoscandia.

The two *S. pictulus* clusters *Stictochironomus* sp. *pictulus* I and *Stictochironomus* sp. *pictulus* II were difficult to tell apart on overall morphology, and telling *S. pictulus* apart from *S. maculipennis* is difficult unless one has both species in hand for comparisons.

The spots on the wing are larger in *S. maculipennis* than in *S. pictulus*, and in some specimens *S. maculipennis* appears to have five spots excluding the one on RM, whereas *S. pictulus* always has four spots excluding the one on RM. The pattern on the legs differ in some specimens as well: *S. pictulus* has a faint third band on the fore tibia, and stronger bands on mid and hind tibia. This third band is sometimes absent in *S. maculipennis*. After assessing the two *S. pictulus* specimens from Sweden, it is clear to me that these have been misidentified and are actually *S. maculipennis*.

There is a unique combination of a few diagnostic characters between *Stictochironomus* sp. *pictulus* I and *Stictochironomus* sp. *pictulus* II. Most notable is the difference in setae on the thorax: *Stictochironomus* sp. *pictulus* I has 12-13 dorsocentrals, 5 prealars, 16 scutellars, whereas *Stictochironomus* sp. *pictulus* II has 20-26 dorsocentrals, 8 prealars and 34-37 scutellars. The shape of the superior volsella is different (Figure 14): *Stictochironomus* sp. *pictulus* I is bulkier and is narrower proximally than *Stictochironomus* sp. *pictulus* II. There are some problems worth assigning. Firstly, the morphological differences could be a result of environmental factors. The specimens of the *Stictochironomus* sp. *pictulus* I cluster were collected mid-May, whereas the specimens of the *Stictochironomus* sp. *pictulus* II cluster were collected in early July. Both *Stictochironomus* sp. *pictulus* II specimens are significantly larger and has more setae than the *Stictochironomus* sp. *pictulus* I specimens. Temperature and availability to food can affect the size of the adult specimens, and thus the number of setae that can fit on the body. Second, the *Stictochironomus* sp. *pictulus* I specimens were in bad condition. Several leg segments and the antennae were missing, and it was impossible to depict the pattern on the wing. The color on the whole body appeared to be faded, but this could also be that the species is much lighter overall than the other species. Third, only two specimens were collected from each cluster, which is not much to base an average morphological analysis on. Lastly, after consulting literature I have not been able to identify which of the clusters is the new species and which is *S. pictulus*. In the end, it appears that the morphological differences are significant, but I recommend collecting and measuring more specimens in the future to solidify the new species, and to decide which one is the new species and which one is *S. pictulus*. Describing the diversity in a way that makes it stable over time requires support by diagnostic morphological characters and genetic characters, or in other words integrative taxonomy.

The last two clusters, *Stictochironomus* sp. *sticticus* Norway and *Stictochironomus* sp. 3TE do not show distinct morphological differences enough of the measurements or observations to call it a unique combination of diagnostic characters. The range of the measurements are greater than in any of the other species. The one notable difference is that sp. 3TE has a faint pattern on the legs and *Stictochironomus* sp. *sticticus* Norway does not. These two clusters could potentially be a case of cryptic species and would need further studies to find morphological differences.

Future priorities

The scope of my thesis was not wide enough to include all life stages. However, in the case of the *S. sticticus* clades, investigating the morphology of the other life stages could reveal if these are two cryptic species or not. I collected and kept some larvae in a small box to have them form a pupa and finally emerge as adults to easily collect all the life stages. Unfortunately, none of the specimens were *Stictochironomus*. The goal of the fieldwork was to get as much experience as possible while also collecting *Stictochironomus* specimens. The location and date for collection were selected based on previous findings of *Stictochironomus*. There could of course be *Stictochironomus* in locations not recorded previously, but since this study is not a study on distribution and biogeography, I chose a few locations to try and find some fresh specimens. I only found adult male and female specimens of *S. rosenschoeldi* in Trøndelag and Finnmark. The field days did not line up with the emergence of the adults. Catching chironomids is easy, because once you start looking they are everywhere. It is not so easy to catch a specific species.

Two hundred and fifty years after the first chironomids were being described, studying, identifying, and describing species is still a challenge. Even experts in the field struggle sometimes. It takes a long time to properly learn what distinguishing characters to look for both between genera and within a genus. Chironomids are small, very fragile and can easily break if preserved on an insect needle. Even though mounting them on microscope slides is much more time consuming, it is a better method for both long time preservation and to study their morphology. Many species are known only from male imagines (Andersen et al., 2013), and even though many scientists are working to include other life stages there is still a long way to go. On the other hand we want to describe the biological diversity as fast as possible so that knowledge can be used in other fields of biology, so there is a fine balance to be found.

Conclusion

In Fennoscandia there are eight species of *Stictochironomus*, three of which are new to science. All the species of *Stictochironomus* were highly supported by molecular delimitation methods. The new species *Stictochironomus* sp. 2TE possesses a unique combination of diagnostic characters, and can thus be described as new to science. The two other species were not possible to delimit morphologically simply from adult male specimens. In order to understand which of the morphologically similar species are the described species *S. sticticus* and *S. pictulus* and which are the two new species, I recommend collecting and measuring more specimens, preferably of all life stages. The original hypothesis of there being three undescribed species in Fennoscandia has been confirmed, although more sampling and morphological measurements are needed in order to solidify the two last species.

References

- Aldhebiani, A. Y. (2018). Species concept and speciation. *Saudi J Biol Sci*, 25(3), 437-440.
<https://doi.org/10.1016/j.sjbs.2017.04.013>
- Andersen, T., Ekrem, T., & Cranston, P. S. (2013). I. The larvae of Holarctic Chironomidae (Diptera) – Introduction. In T. Andersen, Cranston, P. S. & Epler, J. H. (Sci. eds) (Ed.), *The larvae of Chironomidae (Diptera) of the Holarctic region. – Keys and diagnoses. Part 1. Larvae* (Vol. 66, pp. 7-12). Insect Systematics & Evolution, Supplement.
- Anderson, A. M., Stur, E., & Ekrem, T. (2013). Molecular and morphological methods reveal cryptic diversity and three new species of Nearctic Micropsectra (Diptera: Chironomidae). *Freshwater Science*, 32(3), 892-921.
- Armitage, P. D., Cranston, P. S., & Pinder, L. C. V. (1995). *The Chironomidae: Biology and ecology of non-biting midges*. Chapman & Hall.
- Ashe, P., & O'Connor, J. P. (2009). *A world catalogue of Chironomidae (Diptera). Part 1. Buchonomyiinae, Chilenomyiinae, Podonominae, Aphroteniinae, Tanypodinae, Usambaromyiinae, Diamesinae, Prodiamesinae and Telmatogetoninae*. Irish Biogeographical Society & National Museum of Ireland: Dublin.
- Ashe, P., & O'Connor, J. P. (2012). *A World Catalogue of Chironomidae (Diptera), Part 2, Orthocladiinae*. Irish Biogeographical Society & National Museum of Ireland: Dublin.
- Ayres, D. L., Darling, A., Zwickl, D. J., Beerli, P., Holder, M. T., Lewis, P. O., Huelsenbeck, J. P., Ronquist, F., Swofford, D. L., Cummings, M. P., Rambaut, A., & Suchard, M. A. (2012). BEAGLE: An Application Programming Interface and High-Performance Computing Library for Statistical Phylogenetics. *Systematic Biology*, 61(1), 170-173.
<https://doi.org/10.1093/sysbio/syr100>
- Bouckaert, R., Heled, J., Kühnert, D., Vaughan, T., Wu, C.-H., Xie, D., Suchard, M. A., Rambaut, A., & Drummond, A. J. (2014). BEAST 2: A Software Platform for Bayesian Evolutionary Analysis. *PLOS Computational Biology*, 10(4), e1003537.
<https://doi.org/10.1371/journal.pcbi.1003537>
- Bouckaert, R., & Xie, D. (2017). Standard nucleotide substitution models v1. 0.1. In.
- Butler, M. G. (1982). A 7-year life cycle for two Chironomus species in arctic Alaskan tundra ponds (Diptera: Chironomidae). *Canadian Journal of Zoology*, 60(1), 58-70.
<https://doi.org/10.1139/z82-008>
- Cracraft, J. (1989). Speciation and its ontology: the empirical consequences of alternative species concepts for understanding patterns and processes of differentiation. *Speciation and its Consequences*, 28, 59.
- Cranston, P. S., Dillon, M. E., Pinder, L. C. V., & Reiss, F. (1989). 10. The adult males of Chironominae (Diptera: Chironomidae) of the Holarctic region – Keys and diagnoses. In T. s. e. Wiederholm (Ed.), *The adult males of the Chironomidae (Diptera) of the Holarctic region – Keys and diagnoses. Part 3. Adult males* (Vol. 34, pp. 353-502). Entomological Scandinavia Supplement.
- Cranston, P. S., Hardy, N. B., & Morse, G. E. (2012). A dated molecular phylogeny for the Chironomidae (Diptera). *Systematic Entomology*, 37(1), 172-188.
<https://doi.org/https://doi.org/10.1111/j.1365-3113.2011.00603.x>
- Cranston, P. S., Oliver, D. R., & O.A., S. (1989). *(not finished) The adult males of Chironomidae of the Holarctic region – Keys and Diagnoses*.
- Cronquist, A. (1978). Once again, what is a species? Biosystematics in agriculture. Beltsville Symposia in Agr. Res.,
- Darriba, D., Taboada, G. L., Doallo, R., & Posada, D. (2012). ModelTest 2: more models, new heuristics and parallel computing. *Nature Methods*, 9(8), 772.

- Dayrat, B. (2005). Towards integrative taxonomy. *Biological Journal of the Linnean Society*, 85(3), 407-417. <https://doi.org/10.1111/j.1095-8312.2005.00503.x>
- de Jong, Y., Verbeek M, Michelsen V, Bjørn Pde P, Los W, Steeman F, Bailly N, B. C., Chylarecki P, Stloukal E, Hagedorn G, Wetzel FT, Glöckler F, Kroupa A, Korb G, Hoffmann A, Häuser C, Kohlbecker A, Müller A, Güntsch A, . . . L., P. (2014). (not finished) Fauna Europaea – all European animal species on the web. *Biodiversity data journal*(2), e4034. <https://doi.org/10.3897/BDJ.2.e4034>
- De Queiroz, K. (2007). Species Concepts and Species Delimitation. *Systematic Biology*, 56(6), 879-886. <https://doi.org/10.1080/10635150701701083>
- Dobzhansky, T. (1982). *Genetics and the Origin of Species*. Columbia university press.
- Ekrem, T., Stur, E., Orton, M. G., & Adamowicz, S. J. (2018). DNA barcode data reveal biogeographic trends in Arctic non-biting midges. *Genome*, 61(11), 787-796.
- Epler, J. H., Ekrem, T., & Cranston, P. S. (2013). 10. The larvae of Holarctic Chironominae (Diptera: Chironomidae) – Keys and diagnoses. In T. Andersen, Cranston, P. S. & Epler, J. H. (Sci. eds) (Ed.), *The larvae of Chironomidae (Diptera) of the Holarctic region. – Keys and diagnoses. Part I. Larvae* (Vol. 66, pp. 387-556). Insect Systematics & Evolution, Supplement.
- Fabricius, J. C. (1781). *Species insectorum: Exhibentes Differentias Specificas, Synonyma Avctorvm, Loca Natalia, Metamorphosin Adiectis Observationibvs, Descriptionibvs* (Vol. 2). C. E. Bohnii.
- Folmer, O., Black, M., Hoeh, W., Lutz, R., & Vrijenhoek, R. (1994). DNA primers for amplification of mitochondrial cytochrome c oxidase subunit I from diverse metazoan invertebrates. *Molecular Marine Biology and Biotechnology*, 3(5), 294-299.
- Garraffoni, A. R. S., Araújo, T. Q., Lourenço, A. P., Guidi, L., & Balsamo, M. (2019). Integrative taxonomy of a new *Redudasys* species (Gastrotricha: Macrotrichida) sheds light on the invasion of fresh water habitats by macrotrichids. *Scientific Reports*, 9(1), 2067. <https://doi.org/10.1038/s41598-018-38033-0>
- GBIF. *Stictochironomus crassiforceps* (Kieffer, 1922) in GBIF Secretariat (2022). GBIF Backbone Taxonomy. Checklist dataset <https://doi.org/10.15468/39omei> accessed via GBIF.org on 2023-05-29.
- Goetghebuer, M. (1932). Chironomides Palearctiques (Dipteres) conserves au Musee d'Histoire Naturelle de Vienne. *Annalen des Naturhistorischen Museums in Wien*, 91-115.
- Grodhaus, G. (1963). Chironomid midges as a nuisance II: The nature of the nuisance and remarks on its control. *California Vector Views*, 10(5), 27-37.
- Guindon, S., & Gascuel, O. (2003). A simple, fast and accurate method to estimate large phylogenies by maximum-likelihood. *Systematic Biology*, 52, 696-704.
- Kieffer, J. J. (1919). Chironomiden der nordlichen Polarregion. *Entomologische Mitteilungen*, 8, 40-48.
- Kingman, J. F. C. (1982). The coalescent. *Stochastic Processes and their Applications*, 13(3), 235-248. [https://doi.org/https://doi.org/10.1016/0304-4149\(82\)90011-4](https://doi.org/https://doi.org/10.1016/0304-4149(82)90011-4)
- Kumar, S., Stecher, G., Li, M., Knyaz, C., & Tamura, K. (2018). MEGA X: Molecular Evolutionary Genetics Analysis across Computing Platforms. *Mol Biol Evol*, 35(6), 1547-1549. <https://doi.org/10.1093/molbev/msy096>
- Lin, X. L., Stur, E., & Ekrem, T. (2018). Molecular phylogeny and temporal diversification of *Tanytarsus van der Wulp* (Diptera: Chironomidae) support generic synonymies, a new classification and centre of origin. *Systematic Entomology*, 43(4), 659-677. <https://doi.org/https://doi.org/10.1111/syen.12292>
- Lindegaard-Petersen, C. (1971). An ecological investigation of the Chironomidae (Diptera) from a Danish lowland stream (Linding A). *Archiv fur Hydrobiologie*, 69, 465-507.
- Mayr, E. (1999). *Systematics and the origin of species, from the viewpoint of a zoologist*. Harvard University Press.

- Meigen, J. W. (1818). *Systematische Beschreibung der bekannten europäischen zweiflügeligen Insekten*. (Vol. 1).
- Meigen, J. W. (1830). *Systematische Beschreibung der bekannten europäischen zweiflügeligen Insekten*. (Vol. 6).
- Miller, M. A., Pfeiffer, W., & Schwartz, T. (2010). Creating the CIPRES Science Gateway for inference of large phylogenetic trees. 2010 gateway computing environments workshop (GCE),
- Moulton, J. K., & Wiegmann, B. M. (2004). Evolution and phylogenetic utility of CAD (rudimentary) among Mesozoic-aged Eremoneuran Diptera (Insecta). *Molecular Phylogenetics and Evolution*, 31(1), 363-378. [https://doi.org/10.1016/S1055-7903\(03\)00284-7](https://doi.org/10.1016/S1055-7903(03)00284-7)
- Oliver, D. (1971). Life history of the Chironomidae. *Annual review of entomology*, 16(1), 211-230.
- Paradis E, Schliep K (2019). *ape 5.0: an environment for modern phylogenetics and evolutionary analyses in R*. Bioinformatics. Package version 5.7.1. 35, 526-528. <https://doi.org/10.1093/bioinformatics/bty633>.
- Pentinsaari, M., Vos, R., & Mutanen, M. (2017). Algorithmic single-locus species delimitation: effects of sampling effort, variation and nonmonophyly in four methods and 1870 species of beetles. *Molecular Ecology Resources*, 17(3), 393-404. <https://doi.org/https://doi.org/10.1111/1755-0998.12557>
- Pinder, L. C. V. (1978). *A key to the adult males of the British Chironomidae (Diptera) the non-biting midges. Vol I The Key* (Vol. 37). Freshwater Biological Association Scientific Publication.
- Pinder, L. C. V., & Reiss, F. (1986). 10. The pupae of Chironominae (Diptera: Chironomidae) of the Holarctic region – Keys and diagnoses. In T. S. e. Wiederholm (Ed.), *Chironomidae (Diptera) of the Holarctic region. – Keys and diagnoses. Part 2. Pupae* (Vol. 28, pp. 299-456). Entomological Scandinavia Supplement.
- Pons, J., Barraclough, T. G., Gomez-Zurita, J., Cardoso, A., Duran, D. P., Hazell, S., Kamoun, S., Sumlin, W. D., & Vogler, A. P. (2006). Sequence-Based Species Delimitation for the DNA Taxonomy of Undescribed Insects. *Systematic Biology*, 55(4), 595-609. <https://doi.org/10.1080/10635150600852011>
- Porinchu, D. F., & MacDonald, G. M. (2003). The use and application of freshwater midges (Chironomidae: Insecta: Diptera) in geographical research. *Progress in Physical Geography*, 27(3), 378-422.
- Rambaut, A., Drummond, A. J., Xie, D., Baele, G., & Suchard, M. A. (2018). Posterior summarization in Bayesian phylogenetics using Tracer 1.7. *Systematic Biology*, 67(5), 901-904.
- Ratnasingham, S., & Herbert, P., D. N. (2007). BOLD: The Barcode of Life Data System (<http://www.barcodinglife.org>). *Molecular Ecology Notes*, 7(3), 355-364. <https://doi.org/https://doi.org/10.1111/j.1471-8286.2007.01678.x>
- Regier, J. C., Shultz, J. W., Ganley, A. R. D., Hussey, A., Shi, D., Ball, B., Zwick, A., Stajich, J. E., Cummings, M. P., Martin, J. W., & Cunningham, C. W. (2008). Resolving Arthropod Phylogeny: Exploring Phylogenetic Signal within 41 kb of Protein-Coding Nuclear Gene Sequence. *Systematic Biology*, 57(6), 920-938. <https://doi.org/10.1080/10635150802570791>
- Ronquist, F., Teslenko, M., van der Mark, P., Ayres, D. L., Darling, A., Höhna, S., Larget, B., Liu, L., Suchard, M. A., & Huelsenbeck, J. P. (2012). MrBayes 3.2: Efficient Bayesian Phylogenetic Inference and Model Choice Across a Large Model Space. *Systematic Biology*, 61(3), 539-542. <https://doi.org/10.1093/sysbio/sys029>

- R studio: R Core Team (2019). *R: A language and environment for statistical computing*. R Foundation for Statistical Computing, Vienna, Austria. URL <https://www.R-project.org/>.
- Schnell, Ø. A., & Aagaard, K. (1996). Chironomidae - Fjærmygg. In *Limnofauna Norvegica, Katalog over norsk ferskvannsf fauna* (pp. 210-248). Tapir Forlag.
- Song, C., Lin, X.-L., Wang, Q., & Wang, X.-H. (2018). DNA barcodes successfully delimit morphospecies in a superdiverse insect genus. *Zoologica Scripta*, 47(3), 311-324. <https://doi.org/https://doi.org/10.1111/zsc.12284>
- Soponis, A. R. (1977). A revision of the Nearctic species of *Orthocladius* (*Orthocladius*) Van der Wulp (Diptera: Chironomidae). *The Memoirs of the Entomological Society of Canada*, 109(S102), 1-187. <https://doi.org/10.4039/entml09102fv>
- SPLITS package: Thomas Ezard, Tomochika Fujisawa and Tim Barraclough (2021). *splits: SPecies' Limits by Threshold Statistics*. R package version 1.0-20/r56. URL <https://R-Forge.R-project.org/projects/splits/>
- Stamatakis, A. (2014). RAxML version 8: a tool for phylogenetic analysis and post-analysis of large phylogenies. *Bioinformatics*, 30(9), 1312-1313. <https://doi.org/10.1093/bioinformatics/btu033>
- Stur, E., & Ekrem, T. (2020). The Chironomidae (Diptera) of Svalbard and Jan Mayen. *Insects*, 11(3).
- Su, K. F.-Y., Kutty, N. S., & Meier, R. (2008). Morphology versus molecules: the phylogenetic relationships of Sepsidae (Diptera: Cyclorhapha) based on morphology and DNA sequence data from ten genes. *Cladistics*, 24(6), 902-916. <https://doi.org/10.1111/j.1096-0031.2008.00222.x>
- Suchard, M. A., & Rambaut, A. (2009). Many-core algorithms for statistical phylogenetics. *Bioinformatics*, 25(11), 1370-1376.
- Sæther, O. A. (1980). Glossary of chironomid morphology terminology (Diptera: Chironomidae). *Entomol. Scand.*, 14, 1-51.
- Sæther, O. A., & Spies, M. (2010). *Fauna Europaea: Chironomidae*. Retrieved 1. May from www.faunaeur.org
- Thompson, F. C., Evenhuis, N. L., & Sabrosky, C. W. (1999). *Stictochironomus* <http://diptera.org/>
- Tänzler, R., Sagata, K., Surbakti, S., Balke, M., & Riedel, A. (2012). DNA Barcoding for Community Ecology - How to Tackle a Hyperdiverse, Mostly Undescribed Melanesian Fauna. *PLOS ONE*, 7(1), e28832. <https://doi.org/10.1371/journal.pone.0028832>
- Wilkins, J. (2006). Species, kinds, and evolution. *Reports of the National Center for Science Education*, 26(4), 36-45.
- Zetterstedt, J. W. (1838). *Sectio tertia. Diptera. Dipterologis Scandinaviae* (Vol. vi +1,140).

Appendices

Appendix A:

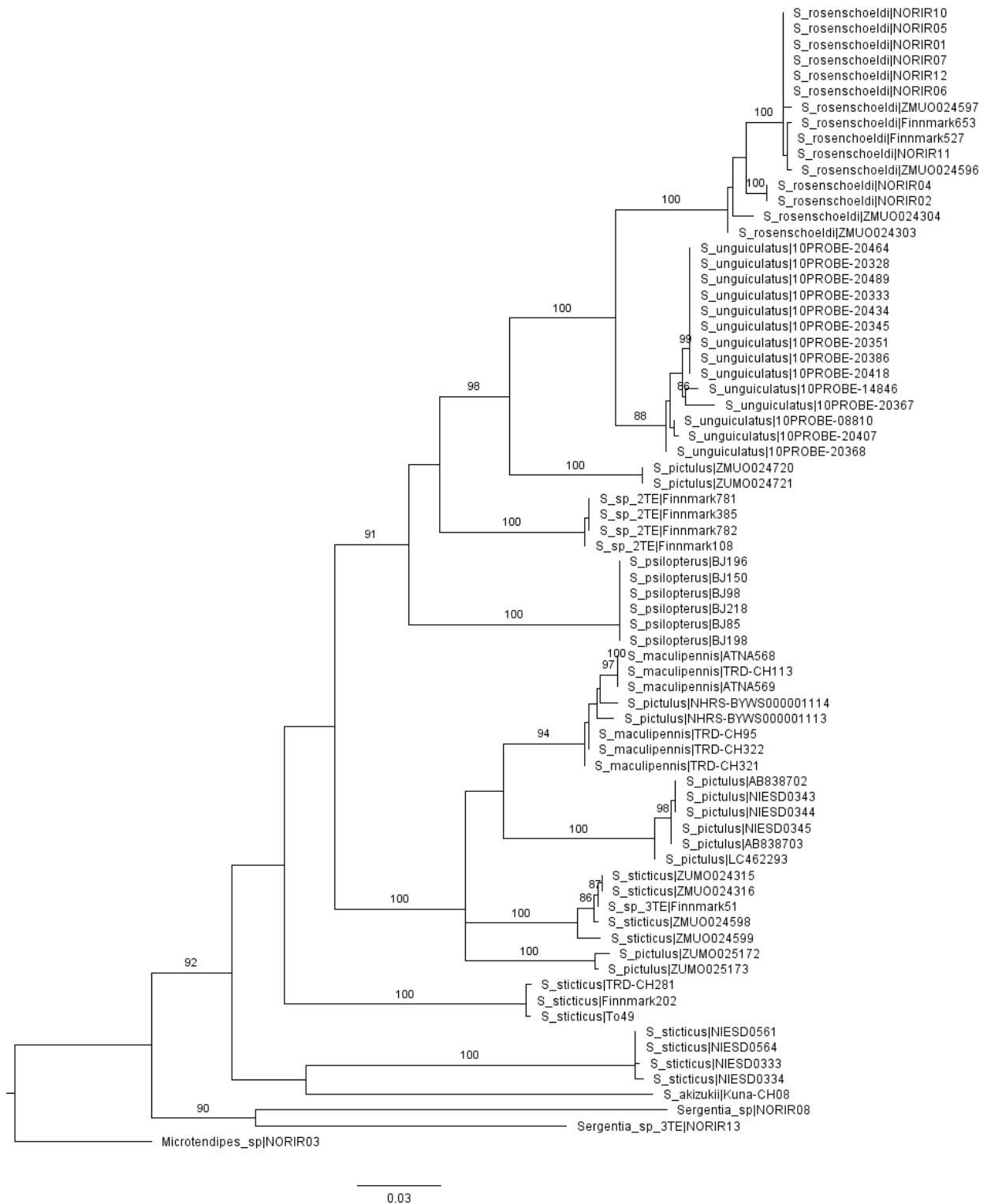


Figure A1 – COI tree from Maximum Likelihood analysis (RAxML) created in CIPRES with default settings. Branch labels are showing bootstrap values less than or equal to 85. Tip are labelled with the morphological species identification, and specimen ID as labelled on microscope slides, or as retrieved from BOLD. Scalebar represents genetic distance.

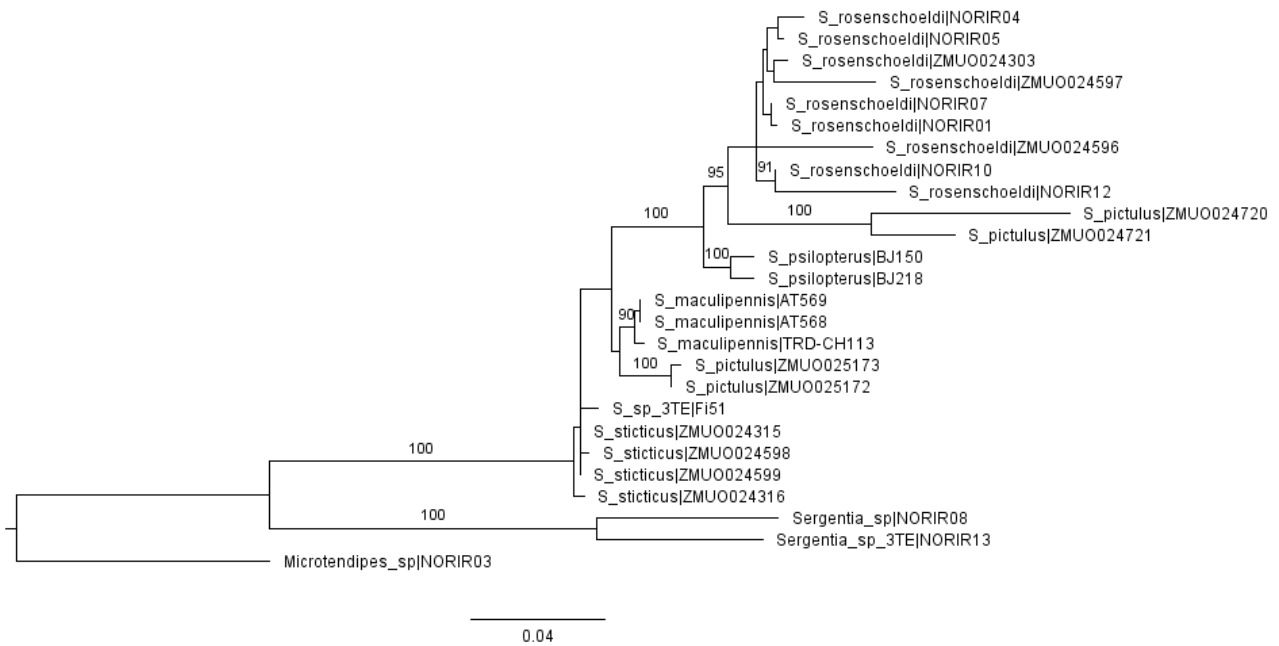


Figure A2 – PGD tree from Maximum Likelihood analysis (RAxML) created in CIPRES with default settings. Branch labels are showing bootstrap values less than or equal to 85. Tip are labelled with the morphological species identification, and specimen ID as labelled on microscope slides, or as retrieved from BOLD. Scalebar represents genetic distance.

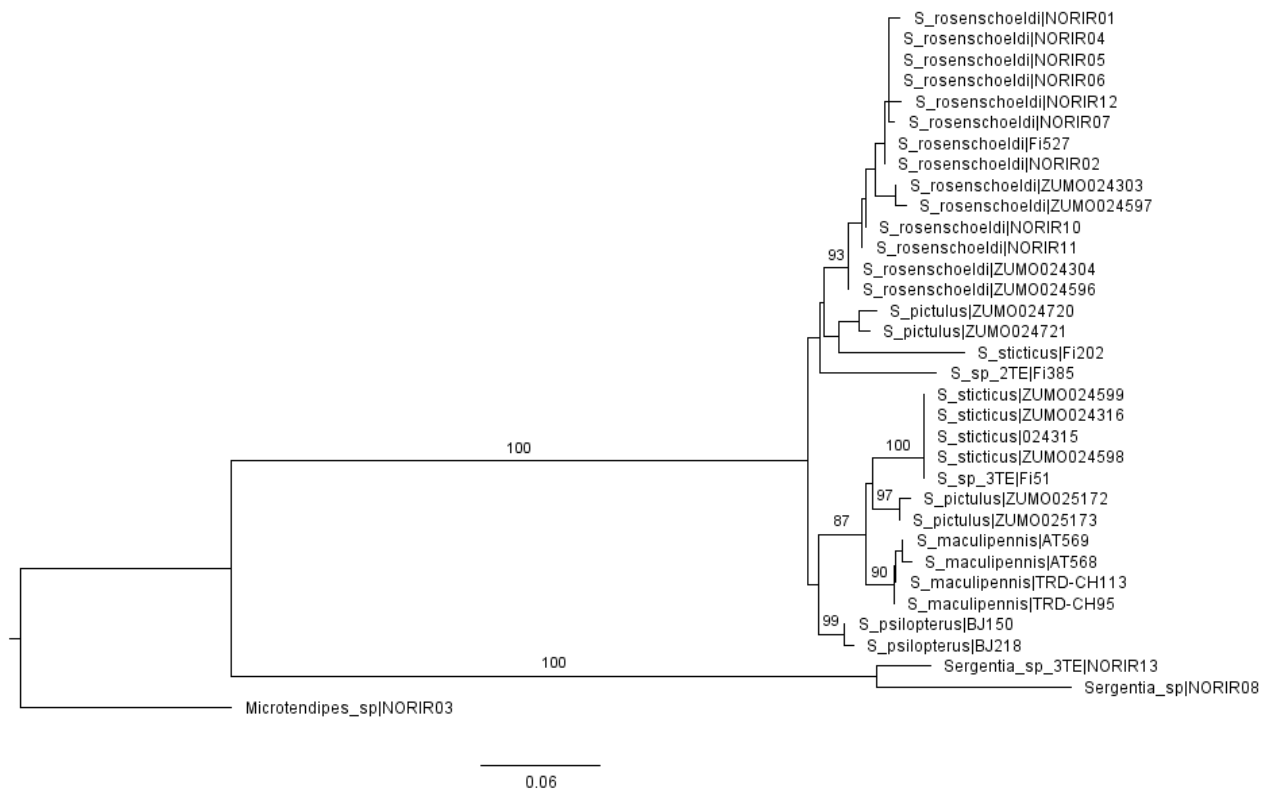
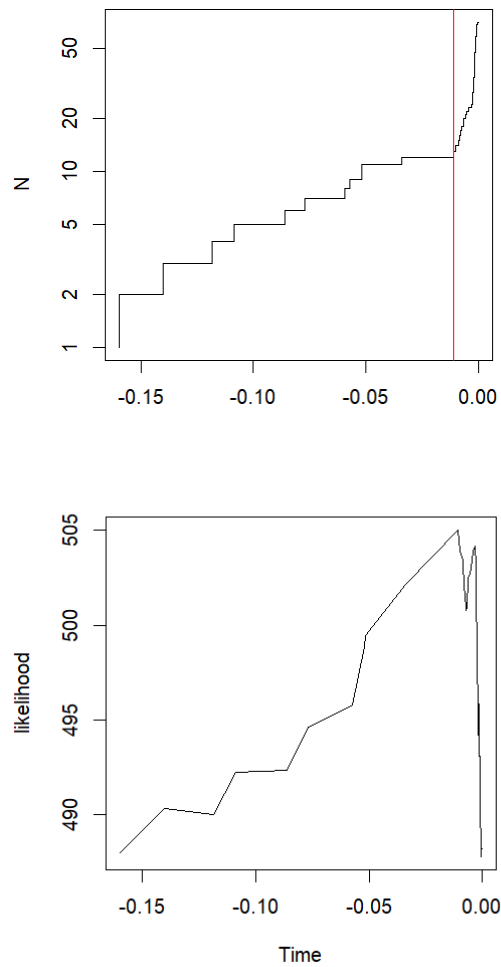


Figure A3 – AATSI tree from Maximum Likelihood analysis (RAxML) created in CIPRES with default settings. Branch labels are showing bootstrap values less than or equal to 85. Tip are labelled with the morphological species identification, and specimen ID as labelled on microscope slides, or as retrieved from BOLD. Scalebar represents genetic distance.



```

> summary(COI_GMYC)
Result of GMYC species delimitation

method: single
likelihood of null model: 487.992
maximum likelihood of
GMYC model: 505.028
likelihood ratio: 34.07209
result of LR test: 3.99337e-08***

number of ML clusters: 11
confidence interval: 11-14

number of ML entities: 12
confidence interval: 12-24

threshold time: -0.01089016

```

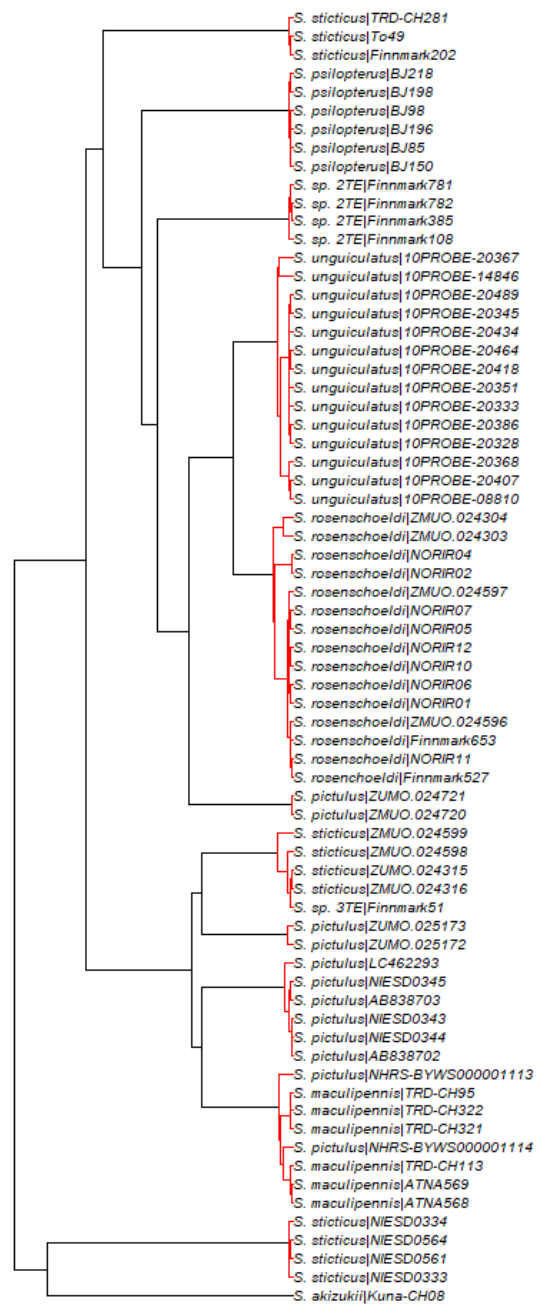
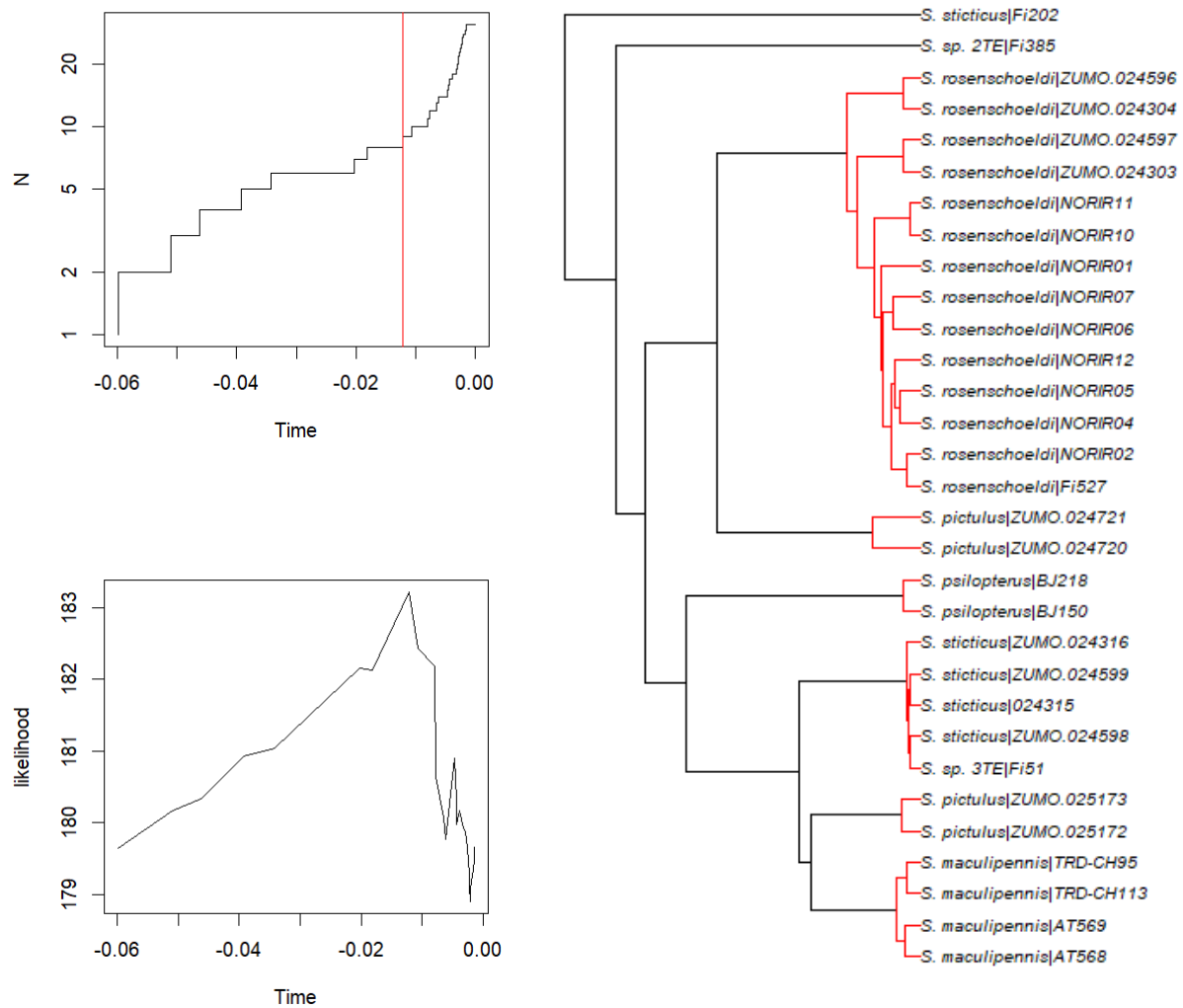


Figure A4 – GMYC results of COI. Line-through-time plot, likelihood function plot, ultrametric tree, summary of results.



```

> summary(AATSI_GMYC)
Result of GMYC species delimitation

method: single
likelihood of null model:179.6438
maximum likelihood of GMYC model: 183.2128
likelihood ratio: 7.138121
result of LR test: 0.02818232*

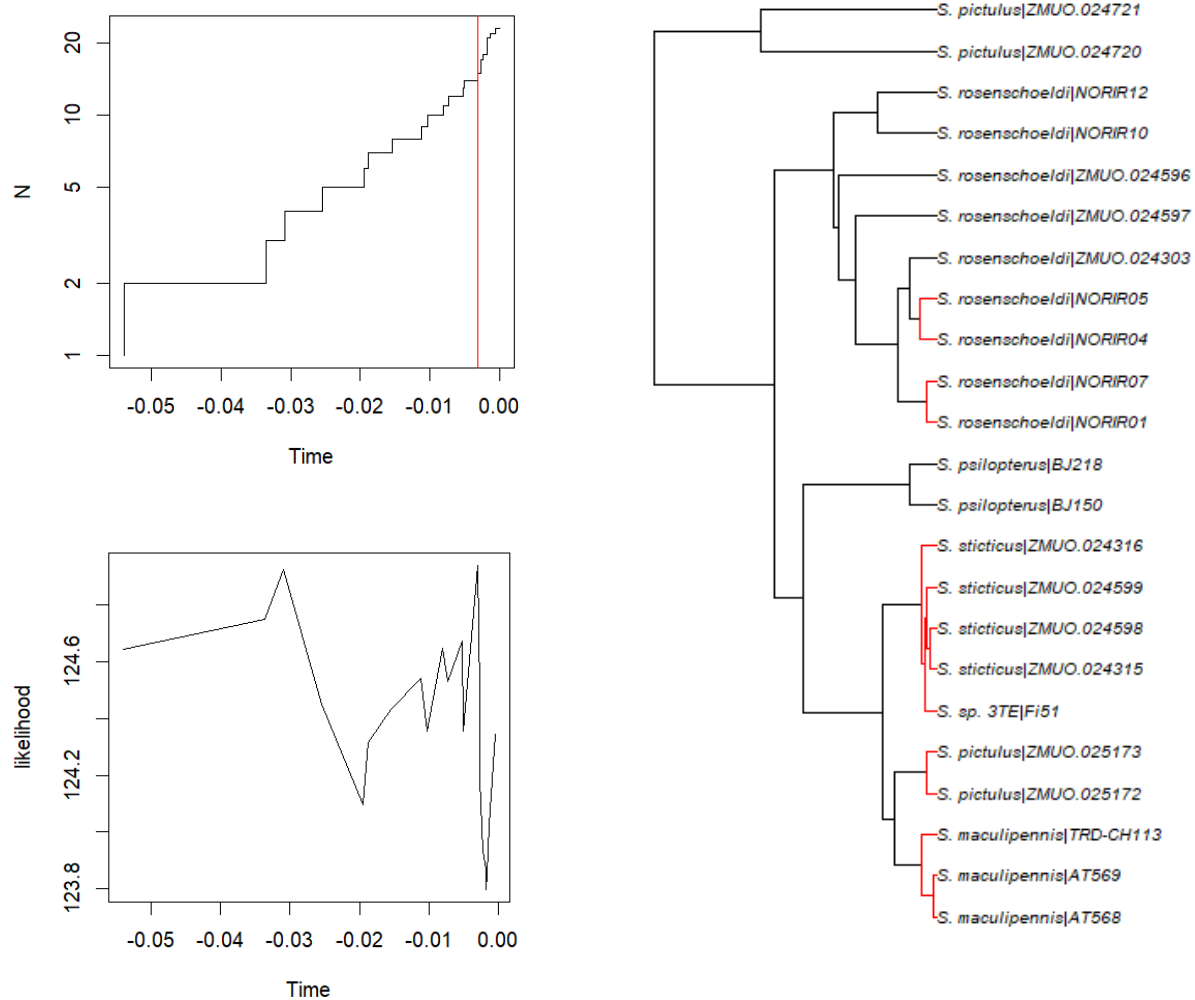
number of ML clusters: 6
confidence interval: 4-8

number of ML entities: 8
confidence interval: 6-10

threshold time: -0.01211189

```

Figure A5 – GMYC results of AATSI. Line-through-time plot, likelihood function plot, ultrametric tree, summary of results.



```

> summary(PGD_GMYC)
Result of GMYC species delimitation

method: single
likelihood of null model: 124.6446
maximum likelihood of GMYC model: 124.939
likelihood ratio: 0.5888832
result of LR test: 0.7449475n.s.

number of ML clusters: 5
confidence interval: 1-6

number of ML entities: 14
confidence interval: 1-22

threshold time: -0.003070986

```

Figure A6 – GMYC results of PGD. Line-through-time plot, likelihood function plot, ultrametric tree, summary of results.

Dorsocentrals	16,0	12,5	23,0	33,5	21,3	22,0	24,0	42,5
Prealars	8,3	5,0	8,0	14,0	8,3	8,5	11,8	19,5
Scutellars	34,7	16,0	35,5	65,0	26,4	37,0	45,0	59,0
Acrostichals*	3,0	15,0	15,0	6,0	9,6	5,0	8,0	8,0
Hypopygium								
Tergite IX	264,0	200,5	247,5	310,5	212,4	281,5	287,6	302,0
Gonostylus	199,3	152,0	198,0	268,0	155,4	218,0	205,8	220,5
Gonocoxite	402,7	301,5	390,0	465,5	333,9	411,0	434,4	425,0
HR	2,020	1,984	1,969	1,738	2,165	1,886	2,111	1,926
Anal point	102,0	84,0	115,5	136,5	94,0	115,0	131,4	120,0
Phallopodeme	128,0	107,5	148,5	165,0	119,6	124,5	150,4	150,0
Transverse sternapodeme	87,7	61,5	69,5	124,0	65,8	95,0	93,8	82,0
Inferior volsella	201,3	147,5	180,5	231,5	152,5	190,0	212,8	219,0
SVo dorsal setae	1,0	1,0	1,0	1,0	1,0	1,0	1,0	1,0
SVo median setae	5,3	4,0	4,5	4,5	4,2	6,0	5,4	5,5
Setae on tergite X	7	6	5,5	8,0	8,4	6,0	5,4	13,5
Qualitative characters								
Superior volsella shape	Variable, in general almost straight with right angle hook	Very bulky stubby almost no hook obtuse	Somewhat bulky, hook acute	Even crescent shape but very blunt apically	Almost straight, often with a neat sharp hook apically	Even or bulky crescent shaped hook	Almost straight to crescent shaped hook	Long thin crescent shaped hook
Dorsocentrals arrangement	1 row	1 row	1 row	3-2 rows	1 row, sometimes two setae in row	1 row, sometimes two setae in row	1 row, sometimes two setae in row	2-1 rows

SV	1,877	1,949	1,906	1,908	1,779	1,855	-	1,888	-	-	-	1,961
Midleg												
Femur	1254	1205	1278	1496	1580	1499	1478	1488	1500	1558	1298	1508
Tibia	1199	1164	1255	1417	1507	1464	1454	1417	1460	1523	1341	1505
Tarsus1	644	669	681	821	889	837	872	812	817	869	1203	874
BR	4,189	3,125	3,026	5,171	3,762	3,400	3,490	-	5,289	4,979	2,581	5,167
Tarsus 2	407	426	416	500	529	514	538	498	-	547	872	570
Tarsus 3	318	332	340	379	405	352	362	352	-	354	681	454
Tarsus 4	210	220	206	257	262	206	205	218	-	220	394	268
Tarsus 5	167	174	161	181	196	178	168	180	-	198	210	195
LR	0,537	0,575	0,543	0,579	0,590	0,572	0,600	0,573	0,560	0,571	0,897	0,581
BV	2,810	2,637	2,862	2,835	2,856	3,040	2,988	2,978	-	2,995	1,781	2,614
SV	3,809	3,541	3,720	3,548	3,472	3,540	3,362	3,578	3,623	3,545	2,194	3,447
Hindleg												
Femur	1409	1387	1467	1703	1776	1760	1699	1722	1697	1805	1704	1692
Tibia	1409	1359	1467	1678	1733	1767	1693	1678	1700	1821	1736	1778
Tarsus 1	976	1016	1027	1217	1265	1248	1316	1192	1276	1271	1184	1314
BR	4,644	6,940	5,396	4,846	4,940	4,193	4,300	-	5,036	5,105	5,055	5,319
Tarsus 2	593	590	635	708	769	786	767	734	786	806	759	795
Tarsus 3	492	499	509	567	618	514	550	546	557	596	612	686
Tarsus 4	283	297	289	337	349	292	280	289	300	308	326	364
Tarsus 5	196	196	183	210	207	219	209	204	-	223	205	234
LR	0,693	0,748	0,700	0,725	0,730	0,706	0,777	0,710	0,751	0,698	0,682	0,739
BV	2,426	2,378	2,451	2,524	2,457	2,637	2,607	2,590	-	2,533	2,431	2,301
SV	2,887	2,703	2,857	2,778	2,774	2,826	2,578	2,852	2,662	2,853	2,905	2,641
Thorax												
Dorsocentrals	23	26	23	18	26	25	18	22	25	30	42	43
Prealars	9	10	8	9	8	11	10	10	13	15	20	19
Scutellars	29	27	25	34	40	53	46	41	40	?	-	59
Acrostichals*	6	-	-	4	6	8	-	-	?	?	?	8
Hypopygium												
Tergite IX	194	238	229	264	299	287	275	261	289	326	302	302
Gonostylus	184	182	148	220	216	197	203	205	205	219	217	224
Gonocoxite	335	363	343	409	413	424	412	440	440	456	395	455
HR	1,821	1,995	2,318	1,859	1,912	2,152	2,030	2,146	2,146	2,082	1,820	2,031
Anal point	99	94	98	115	115	130	127	128	123	149	110	130
Phallapodeme	127	125	134	115	134	131	138	158	155	170	155	145
Transverse sternapodeme	75	73	80	85	105	90	97	106	81	95	70	94
Inferior volsella	156	176	98	203	177	182	218	214	229	221	212	226
SVo dorsal setae	1	1	1	1	1	1	1	1	1	1	1	1
SVo median setae	6	6	3	6	6	5	5	5	4	8	4	7
Setae on tergite X	9	7	8	6	6	5	7	3	5	7	12	15



 **NTNU**

Norwegian University of
Science and Technology